scientific reports

Check for updates

OPEN

Nepenthes pitcher fluid for the green synthesis of silver nanoparticles with biofilm inhibition, anticancer and antioxidant properties

Ovungal Sabira[1], Anthyalam Parambil Ajaykumar[1]✉, Sudhir Rama Varma[2], Kodangattil Narayanan Jayaraj[3]✉, Muddukrishnaiah Kotakonda[4], Praveen Kumar[5], Parvathi Vaikkathillam[5], Valiyaparambil Sivadasan Binitha[6], Alex Philip Alen[7], A. V. Raghu[8] & Koladath Vasu Zeena[1]

This is the first report of silver nanoparticles (AgNPs) synthesis utilizing the pitcher secretion from an insectivorous plant, specifically *Nepenthes ventrata*, through a microwave assisted green synthesis approach. The successful formation of AgNPs was validated through a comprehensive set of analyses, including UV–Vis spectroscopy, Fourier-transform infrared spectroscopy, transmission electron microscopy, DLS analysis and Zeta potential measurements. In addition gas chromatography-high-resolution mass spectrometry and liquid chromatography-high-resolution mass spectrometry analyses were conducted to examine the components present in the pitcher secretion. These analyses aimed to identify the capping and stabilizing agents in the secretion that facilitate the synthesis and stability of AgNPs. The synthesized AgNPs significantly inhibited biofilm formation by *Pseudomonas aeruginosa* PAO1, as demonstrated by Crystal Violet staining and fluorescence microscopy. Additionally, these AgNPs showed promising antioxidant properties through a DPPH radical scavenging assay. Furthermore, the anticancer properties of the AgNPs were analyzed using an MTT assay, which measures cell metabolic activity as an indicator of cell viability, proliferation, and cytotoxicity. Collectively, these findings suggest that the biosynthesized AgNPs possess multifaceted biological applications, showcasing their utility as both antimicrobial and antioxidative agents, and highlighting their potential in medical and environmental applications.

Keywords *Nepenthes ventrata*, Silver nanoparticles, Biofilm inhibition, Pitcher fluid, Anticancer activity and carnivorous plant

The remarkable diversity of the plant kingdom is beautifully illustrated by the vast range of ecological niches that plants have adapted to, spanning from tropical to arctic climates, arid deserts to waterlogged swamps, and from bright sunshine to deep shade. In some of the most nutrient-poor environments, where soil composition is lacking, certain plants have evolved a fascinating survival strategy: insectivory, or more broadly, carnivory. This unique adaptation allows them to thrive by compensating for nutrient deficiencies through the capture and digestion of insects and other small organisms[1–3]. Charles Darwin, widely regarded as the pioneer of evolutionary theory, was the initial researcher to demonstrate that carnivorous plants exude digestive enzymes

[1]Division of Biomaterial Sciences, Department of Zoology, Sree Neelakanta Government Sanskrit College, Pattambi, Palakkad, Kerala, India. [2]Clinical Sciences Department, Centre for Medical and Bio-Allied Health Sciences Research, Ajman University, Ajman, United Arab Emirates. [3]Basic Medical and Dental Sciences Department, Centre for Medical and Bio-Allied Health Sciences Research, Ajman University, Ajman, United Arab Emirates. [4]Department of Pharmaceutics, Jamia Salafiya Pharmacy College, Pulikkal, Kerala, India. [5]Department of Zoology, Government College for Women, Thiruvananthapuram, Kerala, India. [6]Department of Zoology, Sree Narayana College, Nattika, Thrissur, Kerala, India. [7]Department of Botany, Government Victoria College, Palakkad, Kerala, India. [8]Kerala Forest Research Institute, Peechi, Thrissur, Kerala 680653, India. ✉email: ajaykumar@sngscollege.org; j.narayanan@ajman.ac.ae

when exposed to nitrogenous materials. This foundational work, documented in 1875, has been instrumental in shaping contemporary investigations into the biology of carnivorous plants[2,4]. These plants have developed the capacity to catch and digest prey, primarily insects, using specialized traps. This carnivorous adaptation serves as an alternative mechanism for obtaining essential nutrients, such as nitrogen, phosphorus, and potassium[5,6]. Notably, carnivorous plants maintain their ability to fix carbon dioxide and absorb inorganic and organic nutrients from their captured prey, rendering them mixotrophic. This intriguing phenomenon, often referred to as the 'carnivorous syndrome,' is characterized by distinct changes in anatomical structure, glandular features, gene expression, and evolutionary traits. Although carnivorous plants represent a relatively small fraction of the world's flora, approximately 810 species out of the 250,000 flowering plant species[7], they exhibit a remarkable polyphyletic nature, with unique prey-capturing abilities and distinct features.

In the realm of nanotechnology, the quest for innovative and sustainable synthesis methods has led researchers to explore the natural world for inspiration. Among the myriad of biological systems, carnivorous plants, particularly those belonging to the genus Nepenthes, have garnered attention due to their unique digestive mechanisms. These plants produce a cocktail of hydrolytic proteins within their pitcher secretions, including but not limited to proteases, glucanases, chitinases, phosphatases, and nucleases, alongside proteins involved in lipid transfer, pathogenesis, disease resistance, and stress response[8]. This enzymatic diversity, enriched with recent discoveries of enzymes such as amylase, invertase, catalase, and various kinases, ligases, and synthases, emphasizes a complex biochemical environment potentially conducive to the biosynthesis of nanoparticles[9]. The acidic and enzymatically rich nature of Nepenthes' digestive secretions presents an intriguing biological route for the green synthesis of metal nanoparticles, a field increasingly seeking environmentally friendly alternatives. This study aims to support this unique natural process, focusing on the digestive secretions of *Nepenthes ventrata* for the synthesis of silver nanoparticles (AgNPs) from silver nitrate ($AgNO_3$). While the potential of Nepenthes leaf extract in nanoparticle synthesis and its properties has been previously explored[10,11]. The specific application of pitcher secretions, particularly in the context of silver nanoparticle generation, remains largely untapped. Our research is mainly focused on the biosynthetic capabilities of digestive secretions of *N. ventrata* not only in nanoparticle synthesis but also in evaluating the resultant AgNPs in biofilm inhibition and potential anticancer activities. By doing so, this study seeks to bridge a critical gap in the literature, expanding our understanding of the utility of carnivorous plant secretions in nanomaterial production and their implications for medical and environmental applications.

Methodology

Collection of plant secretion

Liquid from the traps was obtained from *Nepenthes ventrata* plants located in Pathanamthitta, Kerala, India (coordinates: 9.34407° N, Longitude 76.77567° E) as depicted in Fig. 1. The *N. ventrata* plant used in this study was identified by the ninth author, who specializes in the plant taxonomy. A voucher specimen has been deposited at the herbarium of the Government Victoria College, Palakkad, Kerala, India, under the voucher ID number GVCH004888. The collection involved both sealed and recently opened pitchers, from which an amount ranging from 5 to 10 mL was gathered directly into sterile plastic tubes. Subsequent to collection, the fluid from the pitchers was subjected to filtration through centrifugation at a speed of 10,000 rpm. Following filtration, the samples were preserved at a temperature of 4 °C until further analysis. These conserved samples were later utilized in the synthesis and analysis of nanoparticles, employing gas chromatography-mass spectrometry (GC–MS) and liquid chromatography-mass spectrometry (LC–MS) techniques for their characterization.

Fig. 1. Insectivorous plant, *Nepenthes ventrata*.

Synthesis of Silver nanoparticles

Silver nanoparticles (AgNPs) were synthesized utilizing the extract from *N. ventrata* traps. Initially, a silver nitrate ($AgNO_3$) solution was prepared at a concentration of 0.01 mM (mM) using deionized water. For the reaction, equal volumes of the gland extract (5 mL) and the $AgNO_3$ solution (5 mL) were mixed together. This mixture was then subjected to heating in a standard household microwave oven (model LG-MS-2029 UW), Specifically, the microwave power (600 W) and exposure time (5 min) were optimized based on preliminary experiments. These parameters were found to ensure uniform size distribution and high stability of the AgNPs, as validated by DLS and zeta potential measurements. A transformation in the colour to a deep brown within this period served as a visual indicator of the AgNPs' formation. Following synthesis, the AgNPs underwent a purification process employing the method of dialysis for an extended period of 72 h. After purification, the AgNPs were stored at room temperature; the nanoparticles were used for subsequent experimental applications.

Nanoparticle characterization

UV–Vis spectroscopy

The synthesis of nanoparticles was confirmed using UV–Vis spectroscopy. The optical absorbance of the nanoparticle solutions was recorded on a PerkinElmer UV/Vis spectrometer, which facilitated the identification of nanoparticle formation.

Fourier-transform infrared spectroscopy (FTIR)

The FTIR technique was employed to elucidate the functional group interactions on the biosynthesized AgNPs, utilizing the *N. ventrata* trap extract as both reducing and stabilizing agent. Comparative FTIR analyses were conducted on the *N. ventrata* trap extract, the biosynthesized AgNPs, and the AgNPs post 72-h dialysis. For this analysis, samples were desiccated, finely pulverized with KBr pellets, and subsequently examined with a PerkinElmer FTIR spectrometer. The resultant spectra were depicted as transmittance percentage against wave number in cm^{-1}.

High-resolution transmission electron microscopy (HR-TEM)

To ascertain the precise size, morphology, and shape of the biologically synthesized AgNPs, HR-TEM analysis was conducted using a Jeol/JEM 2100 instrument. This advanced microscopy technique provided detailed insights into the nanoparticle characteristics.

Zeta potential analysis

The surface charge of the biologically synthesized AgNPs was analyzed through zeta potential measurement. This analysis provided information on the stability and surface charge distribution of the nanoparticles. Together, these characterization techniques offered a comprehensive understanding of the physical and chemical properties of the biosynthesized AgNPs, highlighting their potential for various applications.

Dynamic light scattering (DLS) analysis

Dynamic Light Scattering (DLS) was employed to measure the size distribution of the synthesized silver nanoparticles (AgNPs). The nanoparticles were dispersed in deionized water and sonicated for 10 min to achieve a uniform suspension. Measurements were conducted at room temperature using a Horiba nanoparticle analyzer SZ-100. The samples were placed in disposable cuvettes, and each sample was measured three times to ensure accuracy. The DLS data provided the average particle size and the size distribution profile.

GC-HRMS analysis of pitcher secretion

The of secondary metabolites in *N. ventrata* pitcher secretions was identified by a gas chromatography-high resolution mass spectrometry (GC-HRMS) system, comprising an Agilent 7890 gas chromatograph linked to a Jeol AccuTOF GCv mass spectrometer (Agilent). The GC was fitted with an HP5 capillary column (30 m × 0.25 mm i.d., 0.25 µm film thickness), using helium as the carrier gas at a flow rate of 1 mL/min. The temperature program started at 70 °C, held for 2 min, then increased at 10 °C/min to 300 °C, maintaining for 10 min. Mass spectrometric detection was conducted using Electron Ionization (EI) at 70 eV within a mass range of 35–800 amu and a resolution of 5000, with the GC–MS interface set at 250 °C and detector voltage at 2200 V. Samples were prepared by thawing at room temperature, filtering through a 0.22 µm filter, and the data was analyzed using matching mass spectra with NIST library standards, alongside retention time comparisons.

LC-HR MS analysis of pitcher secretion

The analysis of pitcher fluid secretion was performed using liquid chromatography-mass spectrometry (LC–MS) on a 6550 iFunnel Q-TOF LC/MS system (Agilent Technologies). For sample preparation, the pitcher fluid was collected and filtered through a 0.22 µm membrane filter to eliminate particulate matter, and then diluted with deionized water. Chromatographic separation was achieved using an Agilent ZORBAX Eclipse Plus C18 column (2.1 × 50 mm, 1.8 µm). The mobile phase consisted of 0.1% formic acid in water (Solvent A) and 0.1% formic acid in acetonitrile (Solvent B). The gradient program started with 5% B for 1 min, ramped to 100% B over 8 min, held at 100% B for 10 min, then returned to 5% B over 11 min, with re-equilibration at 5% B for 15 min. The flow rate was maintained at 0.3 mL/min, with an injection volume of 5 µL and a column temperature of 35 °C (Supplementary file 1).

Mass spectrometry was conducted in positive ion mode using a Dual AJS ESI source, with a capillary voltage of 3500 V, nozzle voltage of 1000 V, fragmentor voltage of 175 V, skimmer voltage of 65 V, and octopole RF peak at 750 V. The gas temperature was set at 150 °C with a flow rate of 13 L/min, and the nebulizer pressure was 35 psi. Sheath gas was also at 150 °C with a flow rate of 11 L/min. Data acquisition was performed in

Auto MS/MS mode with a scan range from m/z 60 to 1600, at a rate of 1 spectrum per second for both MS and MS/MS scans. The collision energy was ramped according to the precursor m/z, and precursor selection was based on abundance with active exclusion after one spectrum, released after 0.2 min. Data processing and compound identification were conducted using Agilent MassHunter software, comparing mass spectra with reference standards and databases to ensure accurate characterization of the chemical constituents in the pitcher fluid secretion. This method provided a reliable and detailed analysis of the fluid's composition, crucial for understanding its biochemical properties.

Biofilm inhibition assay of AgNPs

Determination of minimum inhibitory concentration (MIC)

The minimum inhibitory concentration (MIC) of silver nanoparticles (AgNPs) synthesized from the pitcher gland extract of *Nepenthes ventrata* was evaluated against the PAO1 strain of *Pseudomonas aeruginosa* (PAO1). The MIC of AgNPs was determined using the microtiter broth dilution method, according to CLSI guidelines (2018). In each well of a microtiter plate, 50 µL of sterile MHB was added. Then, 50 µL of the AgNP stock solution (50 mg/mL) was introduced into the first well, followed by vertical serial dilutions. Afterward, 50 µL of the bacterial suspension (~ 1×10^6 CFU/mL) was added to each well, and the plate was incubated overnight at 37 °C[12].

Evaluation of Biofilm inhibition by crystal violet assay and Fluorescence Microscopy

The crystal violet (CV) assay is a widely accepted method for assessing bacterial biofilm formation. For biofilm quantification, overnight cultures were initially measured for OD to estimate cell density (~ 1×10^6 CFU/mL). The cell suspensions were then added to microtiter plates along with varying sub-MIC concentrations of AgNPs (6 µg/mL, 12 µg/mL, and 24 µg/mL). The plates were incubated for 24 h at 37 °C. After incubation, biofilms were stained with crystal violet and quantified using an ELISA microplate reader, revealing the impact of AgNPs on biofilm formation[13]. In addition to the Crystal Violet assay, fluorescent microscopy was employed to visually assess the structural integrity of the biofilms following AgNPs treatment. The biofilms were allowed to form under static culture conditions of PAO1 on coverslips, each treated with different concentrations of AgNPs (6 µg/mL, 12 µg/mL, and 24 µg/mL) for 24 h at 37 °C. After incubation, the coverslips were washed with sterile distilled water, stained with 0.01% Acridine Orange, incubated in darkness for 10 min, and then observed using an Axiovert Fluorescent Microscope (ZEISS Vert. A1)[14].

Cytotoxicity assay of AgNPs

A549 lung cancer cell lines were obtained from the National Centre for Cell Sciences (NCCS), Pune, India, and maintained in Dulbecco's Modified Eagle's Medium (DMEM) supplemented with 10% Fetal Bovine Serum (FBS), 100 U/ml penicillin, and 100 µg/ml streptomycin to prevent bacterial contamination. The cells were cultured in a humidified incubator with 5% CO_2 at 37 °C. For the MTT assay, A549 cells were harvested and counted using a hemocytometer, then diluted in DMEM to a density of 1×10^4 cells/ml and seeded into 96-well plates. After an initial 24-h incubation period to allow cell attachment, the cells were treated with various concentrations of biosynthesized silver nanoparticles (AgNPs) from *Nepenthes ventrata* pitcher fluids, ranging from 10 to 50 µg/ml, and incubated at 37 °C in a humidified atmosphere for another 24 h.

Following the treatment period, the medium was replaced with fresh culture medium, and 20 µl of MTT solution (5 mg/ml in PBS) was added to each well. The plates were incubated for an additional 4 h at 37 °C to allow formazan crystal formation by viable cells. The medium was then carefully removed, and 100 µl of concentrated dimethyl sulfoxide (DMSO) was added to each well to dissolve the formazan crystals. Absorbance was measured at 540 nm using a multi-well plate reader, and cell viability was expressed as a percentage of the control (untreated cells). The inhibition of cell proliferation was calculated using the formula:

$$\text{Inhibition of cell proliferation}\,(\%) = (\text{Mean absorbance of the control} - \text{Mean absorbance of the sample}) \times 100.$$

The half-maximal inhibitory concentration (IC_{50}) values, representing the concentration of AgNPs that inhibited cell viability by 50% compared to vehicle control cells, were determined from the dose–response curve. All experiments were performed in triplicate, and the results were expressed as mean ± standard deviation.

Analysis of apoptotic induction using acridine orange/ethidium bromide (AO/EB) dual staining method

The induction of apoptosis in A549 lung cancer cells treated with silver nanoparticles (AgNPs) synthesized using the secretions of the pitcher plant *N. ventrata* was evaluated using the acridine orange/ethidium bromide (AO/EB) dual staining method, following the procedure described by popovic et al. (2006)[15]. A549 cells were seeded at a density of 5×10^4 cells/well in 6-well plates and incubated for 24 h to allow for cell attachment. The cells were then treated with AgNPs at concentrations of 30 µg/ml and 40 µg/ml for 24 h. After the treatment period, the cells were detached using trypsin–EDTA, collected, and washed three times with cold phosphate-buffered saline (PBS) to remove any residual medium and nanoparticles. The washed cells were stained with a mixture of acridine orange (AO) and ethidium bromide (EB), both at a concentration of 100 µg/ml, in a 1:1 ratio for 5 min at room temperature. The stained cells were observed immediately under a fluorescence microscope at 20× magnification. Viable cells exhibited green fluorescence with normal nuclear morphology, early apoptotic cells displayed yellow fluorescence with condensed chromatin, and late apoptotic cells showed orange to red fluorescence with fragmented chromatin. This method allowed for the identification and quantification

of apoptotic and viable cells, providing a reliable assessment of the apoptotic effects induced by the AgNPs synthesized using *Nepenthes ventrata* secretions. All observations were recorded and analyzed to determine the extent of apoptosis in treated cells compared to untreated controls.

Environmental toxicity studies

Fresh *Allium cepa* (onion) bulbs were chosen to investigate the genotoxic potential of AgNPs synthesized from the Pitcher fluid. Equal-sized bulbs (2n = 16) were exposed to varying concentrations of AgNPs solutions (100 µg, 200 µg, 300 µg, 400 µg, and 500 µg), while control bulbs were incubated in distilled water. Hydrogen peroxide (H_2O_2) served as the positive control, and a nanoparticle-free solvent was used as the negative control. The bulbs were allowed to develop roots measuring 2–3 cm in length. These roots were then excised and processed for chromosomal aberration studies using the squash method. Root tips were stained with methylene blue, and chromosomal analysis was conducted by examining 1000 cells from the three most optimal preparations for each treatment under a LEICA ICC50E compound microscope[16].

Results and discussion

In this study, silver nanoparticles (AgNPs) were successfully synthesized using the secretions of the insectivorous plant *N. ventrata*. Comprehensive chemical characterizations, including UV–Vis spectroscopy, FTIR, TEM, zeta potential, and DLS analysis, confirmed the formation and stability of the AgNPs. These nanoparticles exhibited significant antibacterial, anticancer, and radical scavenging properties. The bioactivity observed can be linked to the diverse array of compounds present in the pitcher fluid, as revealed through LC-HRMS and GC–HRMS analyses, highlighting the potential of Nepenthes ventrata as a source for biologically active AgNPs.

UV analysis

During the green synthesis of AgNPs using the liquid extract from the pitcher part of the insectivorous plant *N. ventrata*, a noticeable colour change in the solution from colourless to dark brown indicates the presence of AgNPs Fig. 2a. The results of the UV–Vis analysis are presented in Fig. 2b. As seen in the spectrum, a strong peak at 450 nm indicates the Surface Plasmon Resonance peak that arises from the oscillations of surface electrons of silver metal in an electromagnetic environment. Thus, the formation of AgNPs using the defensive secretion of *N. ventrata* is confirmed. Which shows agreement with previous results of green synthesised AgNPs[17,18].

FTIR analysis

In the infrared spectroscopy analysis of both the liquid extracts from the pitcher part of *N. ventrata* and the silver nanoparticles (AgNPs) synthesized using these extracts, distinct wave numbers corresponding to specific functional groups were identified Fig. 3, revealing insights into the chemical interactions potentially responsible for nanoparticle synthesis and stabilization. The *N. ventrata* extract showed peaks at 2918 cm^{-1}, 2423 cm^{-1}, 1626 cm^{-1}, 1384 cm^{-1}, and 1066 cm^{-1}, indicating the presence of C–H stretching in alkanes, a peak possibly related to atmospheric CO_2, C=C or C=O stretching in alkenes or amides, and C-O stretching in alcohols, ethers, or esters, respectively. Similarly, synthesized AgNPs displayed peaks at 2925 cm^{-1}, 2426 cm^{-1}, 1634 cm^{-1}, 1384 cm^{-1}, 1054 cm^{-1}, 875 cm^{-1}, and 470 cm^{-1}, corresponding to C–H stretching in alkanes, an undefined feature potentially related to CO_2, C=C or C=O stretching, C–H bending in alkanes, C–O stretching, C–H bending in alkenes, and out-of-plane bending or metal–oxygen bonds, respectively[19–21].

In the green synthesis of silver nanoparticles (AgNPs) using *N. ventrata* extracts, stabilization and capping mechanisms are governed by intricate biochemical interactions between organic molecules in the plant secretions and the nanoparticle surfaces. Hydrocarbon chains, evidenced by IR spectral peaks at 2925 cm^{-1} and 875 cm^{-1}, provide a hydrophobic layer that prevents nanoparticle aggregation through steric barriers[22]. Oxygen-containing

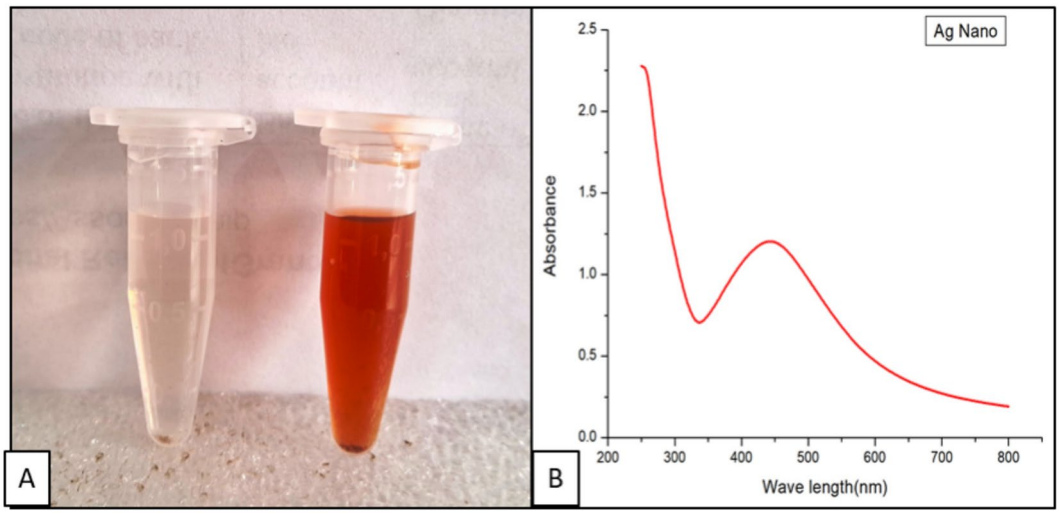

Figure. 2.. Primary characterisation of AgNPs (**a**) Colour change after MW irradiation (**b**) UV–Vis spectrum.

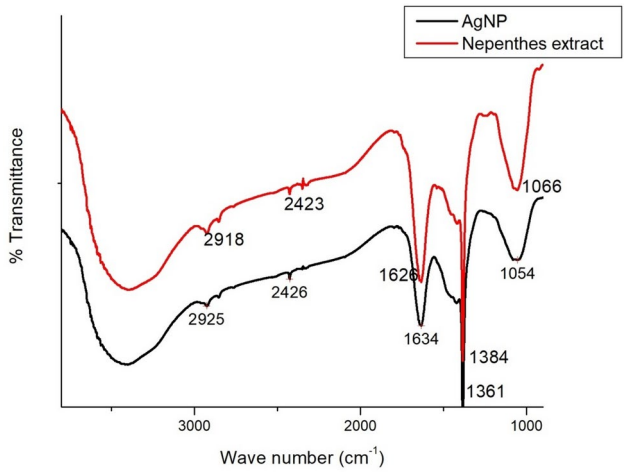

Fig. 3. FTIR spectra of nepenthes extract and extract mediated AgNPs.

Wave number (cm^{-1})	Functional group in Nepenthes extract	Functional group in silver nanoparticles	Shared functional group
2918/2925	C–H stretching in alkanes	C–H stretching in alkanes	C–H stretching in alkanes
2423/2426	Possibly atmospheric CO_2 or noise	Possibly atmospheric CO_2 or noise	Atmospheric CO_2 or noise
1626/1634	C=C stretching in alkenes or C=O stretching in amides	C=C stretching in alkenes or C=O stretching in amides	C=C or C=O stretching
1384	C–H bending in alkanes	C–H bending in alkanes	C–H bending in alkanes
1066/1054	C–O stretching in alcohols, ethers, or esters	C–O stretching in alcohols, ethers, or esters	C–O stretching
875	Not present	C–H bending in alkenes	C–H bending in alkenes (Nanoparticles only)
470	Not present	Out-of-plane bending or metal–oxygen bonds	Metal–oxygen bonds (Nanoparticles only)

Table 1. Comparative analysis of the infrared (IR) spectra for both the liquid extract from *N. ventrata* and the synthesized silver nanoparticles (AgNPs).

groups such as alcohols, ethers, and esters, indicated by C–O stretching at 1054 cm^{-1} and 1066 cm^{-1}, interact with the nanoparticle surface through coordination bonds or hydrogen bonding, forming a protective layer that enhances biocompatibility and functionality[23]. Additionally, amide linkages, suggested by the peak at 1634 cm^{-1}, stabilize the nanoparticles by binding to the surface via nitrogen's lone pair electrons, forming a robust layer that prevents oxidation[24]. These interactions underscore a multifaceted approach where *N. ventrata* extracts not only facilitate the reduction and synthesis of nanoparticles but also impart crucial stability and functionality, highlighting the potential of plant extracts in sustainable nanoparticle production for diverse applications.

The Table 1 provides a comparative analysis of the infrared (IR) spectra for both the liquid extract from *N. ventrata* and the synthesized AgNPs. The comparative analysis of functional groups in Nepenthes pitcher fluid and the silver nanoparticles (AgNPs) synthesized from it shows both similarities and differences that highlight the transformation during synthesis. Functional groups such as C–H stretching in alkanes (2918/2925 cm^{-1}), C=C or C=O stretching (1626/1634 cm^{-1}), C–H bending in alkanes (1384 cm^{-1}), and C–O stretching in alcohols, ethers, or esters (1066/1054 cm^{-1}) are present in both the pitcher fluid and AgNPs.

Interpretation of IR spectra based on LC–MS data and identified metabolites

The IR spectra of the AgNPs synthesized using pitcher secretion, compared to the Nepenthes secretion alone; provide valuable insights into the functional groups involved in the reduction process (Fig. 3). The broad peak between 3200 and 3600 cm^{-1}, indicating O–H stretching vibrations, is significant in the pitcher secretion, suggesting the presence of hydroxyl groups from metabolites such as evoxanthidine, sarmentosin, 3beta,6beta-dihydroxynortropane, 3-furanmethanol glucoside, and droxidopa. These hydroxyl groups are crucial in reducing Ag^{+} ions to AgNPs[25]. Peaks around 2918 and 2925 cm^{-1}, corresponding to C–H stretching vibrations, indicate the presence of aliphatic chains from fatty acids or similar compounds, which play a role during the reduction process[26]. The peaks at 2423 and 2426 cm^{-1}, associated with C≡C or C≡N stretching, suggest the presence of nitrogen-containing compounds like sarmentosin and D-tryptophan. The C=O stretching vibrations at 1626 and 1634 cm^{-1} indicate carbonyl groups, pointing to metabolites such as lycoperdic acid and suberylglycine. Aromatic compounds like evoxanthidine and D-tryptophan are indicated by the peak around 1384 cm^{-1}, corresponding to C=C stretching vibrations. Finally, the peaks at 1054 and 1066 cm^{-1}, representing C-O stretching and O–H bending vibrations, further confirm the presence of hydroxyl and carboxyl groups from the identified

metabolites, which are essential for the reduction and stabilization of AgNPs[27]. These findings collectively show that the functional groups from various metabolites in Nepenthes secretion, including hydroxyl, carbonyl, and aromatic groups, are integral to the synthesis of silver nanoparticles.

DLS analysis of AgNPs

Dynamics Light Scattering (DLS) was used to examine the size distribution of silver nanoparticles (AgNPs) that were produced by utilising *Nepenthes ventrata* pitcher secretion. The findings show a monodispersed distribution of nanoparticles with a restricted size range, as seen in Fig. 4, which indicates a high level of size uniformity in the nanoparticles. The bulk of the synthesised AgNPs, as indicated by the frequency distribution curve, have a size centred around 20–30 nm, with a peak frequency at about 25 nm (Fig. 3). The findings are corroborated by the inset histogram, which displays a uniform size distribution devoid of notable aggregation.

Zeta potential analysis

The zeta potential of the AgNPs synthesized using pitcher fluid secretion was evaluated to determine their colloidal stability. The analysis, depicted in Fig. 5, reveals a peak zeta potential value of -17.5 mV. This negative zeta potential suggest stability of the AgNPs as the negative charge creates electrostatic repulsion that helps to prevent particle aggregation. Additionally, the electrophoretic mobility was found to be -0.000135 cm^2/Vs. The mean zeta potential value of -17.5 mV is indicative of a reasonably stable colloidal system, which is essential for the practical application of these nanoparticles. The single peak in the zeta potential distribution further indicates the uniformity and consistent stability of the synthesized AgNPs.

The synthesis of AgNPs using *N. ventrata* pitcher secretion demonstrates a promising application of biogenic methods in green nanotechnology. The secretion contains a diverse array of compounds including evoxanthidine, a phenolic compound known for its effective electron donation capabilities which facilitate the reduction of Ag^{+} to Ag^{0} and stabilize the nanoparticles through aromatic interactions[28]. Alkaloids such as sarmentosin and 3beta,6beta-dihydroxynortropane contribute to both reduction and stabilization processes via nitrogen-mediated chelation[29]. The amino acid derivative D-Tryptophan, with its indole ring, provides additional electron-donating capacity and helps stabilize the nanoparticles with its amine and carboxyl groups. The glucoside 3-furanmethanol glucoside reduces silver ions through hydroxyl group-driven electron transfer and enhances nanoparticle solubility and stability via its sugar moieties[30]. Furthermore, droxidopa, a catecholamine, participates in the redox reactions essential for reducing metal ions and stabilizing nanoparticles through its catechol group, showcasing a significant contribution to the robustness of the nanoparticle synthesis process[31]. In this secretion, several compounds have been identified with strong reducing properties that may facilitate the reduction of silver nitrate to AgNPs, including evoxanthidine, D-tryptophan, and droxidopa. Each of these compounds possesses chemical groups capable of donating electrons to silver ions, effectively reducing them to elemental silver. Collectively, these compounds illustrate the multifaceted roles of pitcher secretion components in nanoparticle synthesis, highlighting the potential of plant-based extracts in producing environmentally friendly and stable nanoparticles, which could revolutionize applications in medicine and electronics.

HR-TEM

High Resolution Transmission electron microscopy (HR-TEM) analysis revealed that the synthesized silver nanoparticles (AgNPs) possess a predominantly spherical morphology. The TEM images clearly showed uniform, well-dispersed nanoparticles with a size range between 20–30 nm (Fig. 6). This size range is critical for their enhanced surface area, which directly influences the nanoparticles' reactivity and interaction with biological systems. The spherical shape and nanoscale dimensions are particularly favourable for applications in areas such as drug delivery, catalysis, and biomedical interventions, as they contribute to the stability, solubility, and

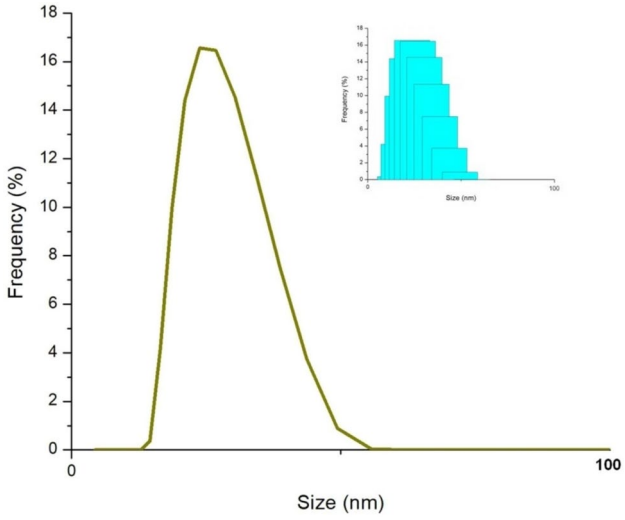

Fig. 4. DLS frequency distribution curve.

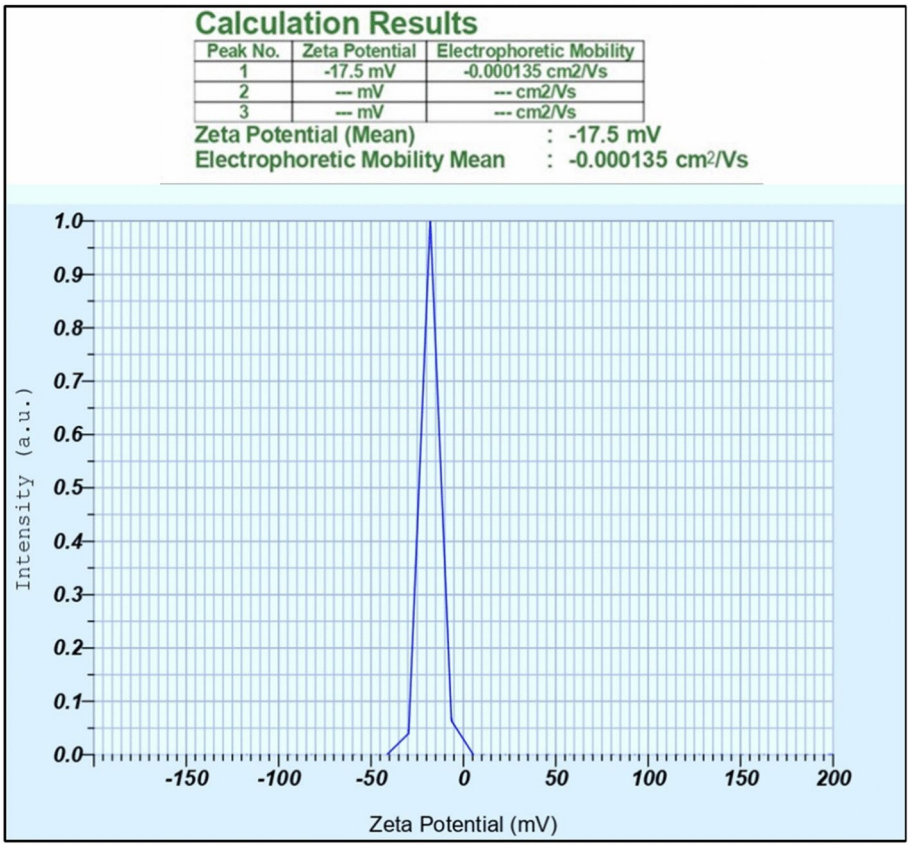

Figure. 5.. Zeta potential showing AgNPs surface charge.

bioavailability of the nanoparticles. Additionally, the narrow size distribution observed through TEM analysis suggests a controlled and consistent synthesis process, further supporting the effectiveness of using *N. ventrata* secretions as a natural reducing and stabilizing agent in nanoparticle fabrication.

GC-HRMS analysis of pitcher secretion

The GC-HRMS analysis of *N. ventrata* pitcher secretion showed the presence of various metabolites (Fig. 7). The major compounds identified include Octadecanoic Acid, 1-[[(1-oxohexadecyl) oxy]methyl]-1,2-ethanediyl Ester (C55H106O6) with a molecular mass of 862 Da. Additionally, Octadecanoic Acid, 2-[(1-oxohexadecyl)oxy]-1-[[(1-oxohexadecyl)oxy] methyl]ethyl Ester (C53H102O6) with a molecular mass of 834 Da and Octadecanoic Acid, 3-[(1-oxohexadecyl)oxy]-2-[(1-oxotetradecyl)oxy]propyl Ester (C51H98O6) with a molecular mass of 806 Da were also identified. Another important compound was 10-Acetoxy-2-hydroxy-1,2,6a,6b,9,9,12a-heptamethyl-1,3,4,5,6,6a,6b,7,8,8a,9,10,11,12,12a,12b,13,14b-octadecahydro-2H-picene (C33H52O5) with a molecular mass of 528 Da.

LC-HRMS analysis of pitcher fluid

In this study, LC-HRMS analysis identified several compounds from the pitcher fluids of the insectivorous plant *N. ventrata* (Fig. 8 and Table 2). Among the compounds detected, evoxanthidine was found with a mass-to-charge ratio (m/z) of 270.0763, known for its defensive properties, helping the plant protect itself from pathogens and pests. Hypoglycin B, identified at m/z 270.1214, plays a crucial role in energy metabolism and possibly deters herbivores due to its toxicity[32]. Lycoperdic acid, found with an m/z of 217.0585, contributes to microbial activity within the pitcher fluid, aiding in the breakdown of prey and maintaining microbial balance[33]. Sarmentosin, detected at m/z 275.0999, aids in nutrient absorption and enhances the plant's defence mechanisms by contributing to the formation of defensive secondary metabolites[34]. 3beta,6beta-Dihydroxynortropane, identified at m/z 144.1006, is involved in attracting prey and assisting in the digestion process through its enzymatic activity[35]. Suberylglycine, found at m/z 254.0996, contributes to the enzymatic activities of pitcher plants, aiding in the breakdown of prey and nutrient absorption[36]. D-Tryptophan, detected with an m/z of 204.0875, is involved in nitrogen metabolism, helping the plant assimilate nitrogen from its prey[37]. Methyl N-methylanthranilate, identified at m/z 188.0688, has antimicrobial properties, protecting the plant from microbial infections[38]. Axisothiocyanate 3, detected with an m/z of 264.1778, contributes to the plant's chemical defense against pests and pathogens[39]. Buthionine sulfoximine, found at m/z 245.093, plays a role in glutathione metabolism, helping the plant manage oxidative stress and maintain cellular health[40].

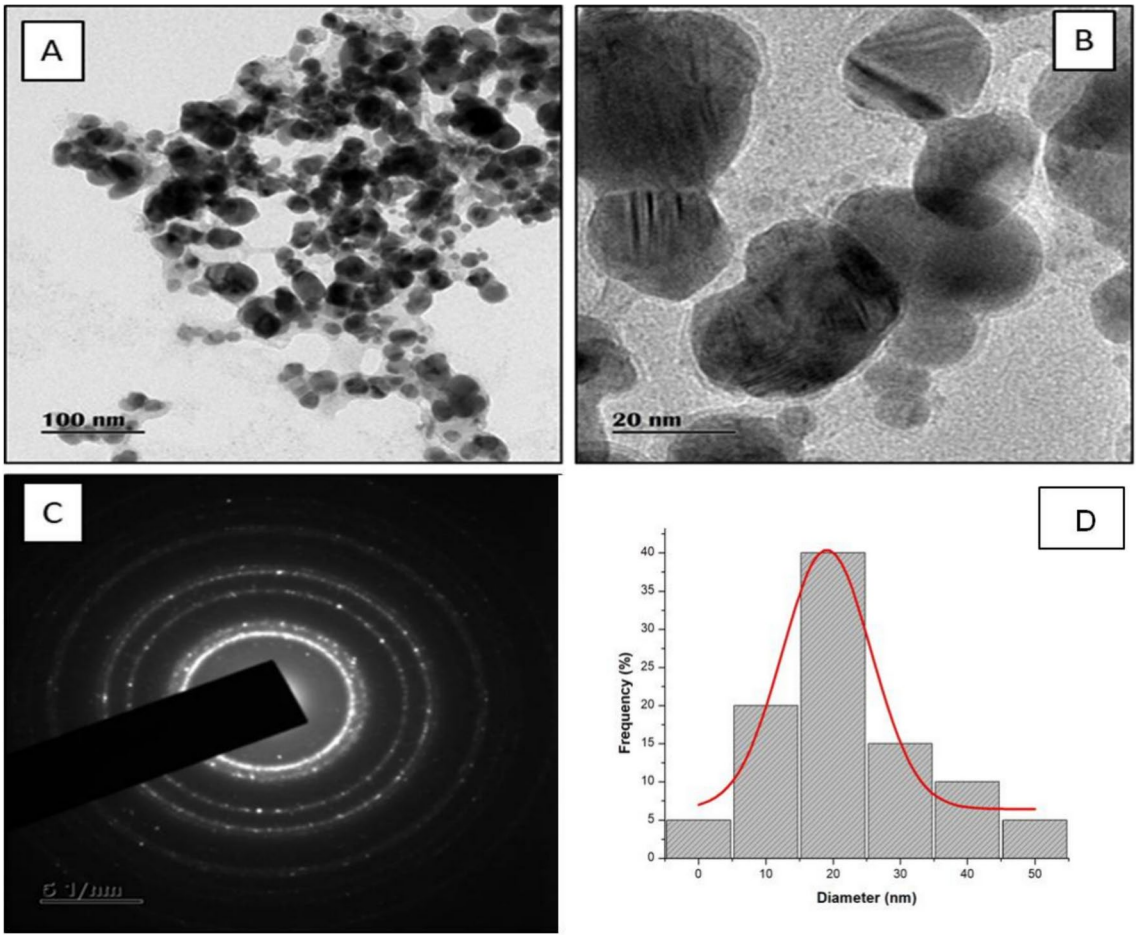

Fig. 6. HR-TEM data of AgNPs.

Additional plant metabolites identified from the pitcher fluids include 3-furanmethanol glucoside, detected with an m/z of 283.0786, which is involved in various metabolic processes within the plant, including energy metabolism and stress responses. N-acetyl-L-2-amino-6-oxopimelate, identified at m/z 254.0999, is a metabolite involved in amino acid metabolism, contributing to protein synthesis and overall plant growth[41]. Fospropofol, detected at m/z 293.1106, contributes to the biochemical pathways of the plant, aiding in various metabolic functions[42]. Droxidopa, found with an m/z of 244.0944, is crucial for plant defense mechanisms and stress responses, helping the plant adapt to environmental challenges[43]. 2-hydroxy-3-carboxy-6-oxo-7-methylocta-2,4-dienoate, detected at m/z 251.0524, plays a significant role in the plant's secondary metabolism, contributing to the synthesis of essential compounds for growth and defense[44]. The analysis also identified additional compounds such as N5-(4-methoxybenzyl)glutamine, detected at m/z 266.1269, involved in metabolic processes and defense mechanisms within the plant[45]. 2-hexylbenzothiazole, identified at m/z 222.1037, helps defend against microbial pathogens, maintaining the plant's health. Maculosin, found at m/z 260.0896, is known for its role in secondary metabolism, aiding in the production of defensive compounds[46]. N-carboxyacetyl-D-phenylalanine, identified at m/z 254.0897, plays a significant role in amino acid metabolism, contributing to protein synthesis and plant development. Alitame, detected at m/z 331.1525, plays a role in various metabolic pathways, including stress responses and adaptation to environmental conditions[47]. These findings highlight the complex chemical composition of *N. ventrata* pitcher fluids and their significant roles in plant defense, prey digestion, and overall metabolic processes. The identified compounds not only enhance our understanding of the plant's biology but also offer potential applications in biotechnology and medicine. Further studies on these compounds can provide deeper insights into their specific functions and potential benefits.

The metabolites identified through HR-LCMS analysis that exhibit stronger reducing properties compared to other detected compounds are Evoxanthidine (Phenolic Compound), Sarmentosin (Alkaloid), 3beta,6beta-Dihydroxynortropane (Alkaloid), D-Tryptophan (Amino Acid Derivative), 3-furanmethanol glucoside (Glucoside), and Droxidopa (Catecholamine) (Table 3). Due to their strong redox potential and ability to promote electron transfer during the formation of silver nanoparticles, these metabolites are believed to be primarily responsible for reducing silver nitrate into silver nanoparticles (Fig. 9). Their unique chemical structures enhance their reducing capability, making them key contributors to the natural synthesis process observed in the pitcher secretion of *N. ventrata*.

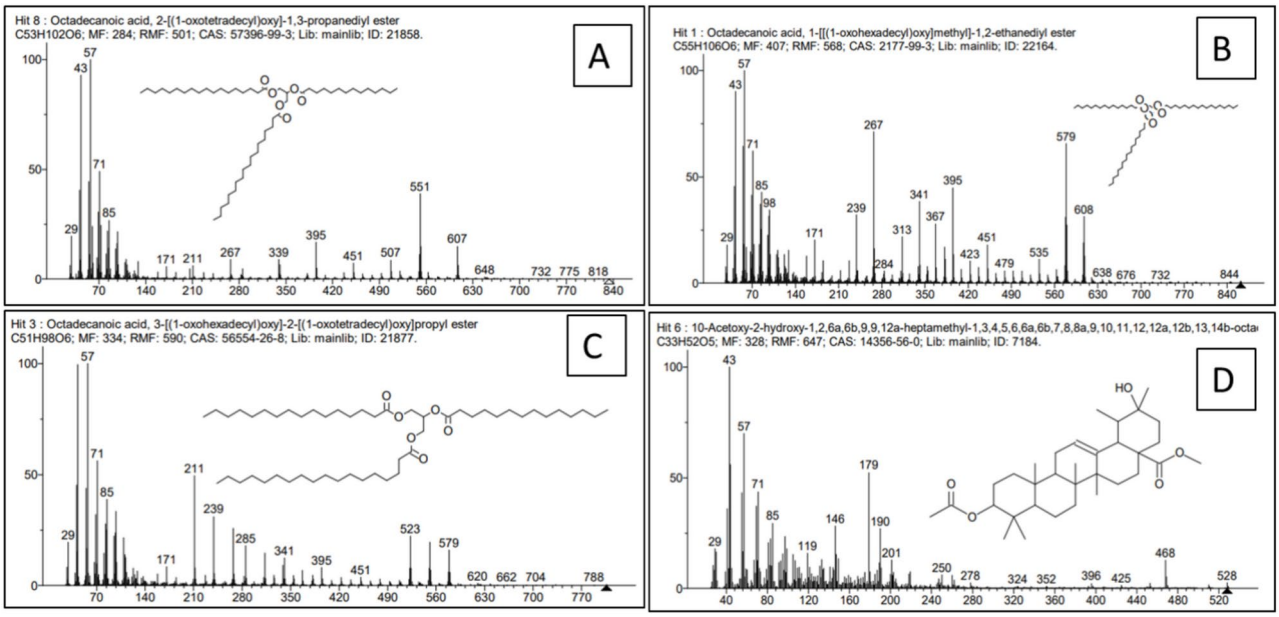

Fig. 7. GC-HRMS analysis identified four compounds in the pitcher secretion of *N. ventrata*: Compound (**A**) Octadecanoic Acid, 1-[[(1-oxohexadecyl) oxy]methyl]-1,2-ethanediyl Ester; Compound (**B**) Octadecanoic Acid, 2-[(1-oxohexadecyl)oxy]-1-[[(1-oxohexadecyl)oxy] methyl]ethyl Ester; Compound (**C**) Octadecanoic Acid, 3-[(1-oxohexadecyl)oxy]-2-[(1-oxotetradecyl)oxy]propyl Ester; and Compound (**D**) 10-Acetoxy-2-hydroxy-1,2,6a,6b,9,9,12a-heptamethyl-1,3,4,5,6,6a,6b,7,8,8a,9,10,11,12,12a,12b,13,14b-octadecahydro-2H-picene.

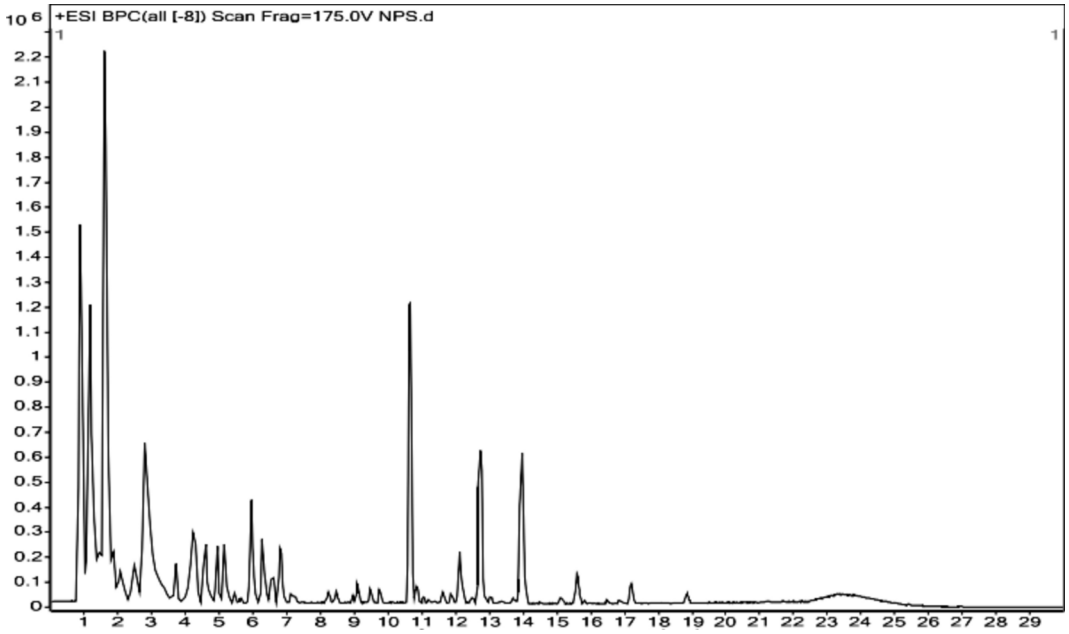

Fig. 8. LC-HRMS profile of extract of pitcher fluid of *N. vengtrata.*

Anti-bacterial and anti-biofilm efficacy of AgNPs synthesized using *N. ventrata* secretion

The antibacterial efficacy of AgNPs was assessed against PAO1, yielding a low MIC of 48 µg/mL. Consistent with these findings, multiple studies have demonstrated the potent antimicrobial activity of AgNPs, reporting similarly low MIC values against a range of bacterial species, including *P. aeruginosa*[48,49]. The anti-biofilm activity of AgNPs synthesized from the secretion of *N. ventrata* was evaluated against *Pseudomonas aeruginosa* PAO1 using a 24-h crystal violet assay. The results demonstrated a pronounced reduction in biofilm formation with increasing concentrations of AgNPs, revealing a potent dose-dependent antibiofilm activity (Fig. 10). At a

Sl. No	Name of the compound	Mass-to-charge ratio (m/z)	Reducing properties for synthesizing AgNPs
1	Evoxanthidine	270.0763	Moderate reducing agent due to its phenolic structure
2	Hypoglycin B	270.1214	Weak reducing properties, primarily a metabolic regulator
3	Lycoperdic acid	217.0585	Moderate reducing agent, contributes to microbial activity
4	Sarmentosin	275.0999	Strong reducing agent due to hydroxyl and amine groups
5	3beta,6beta-Dihydroxynortropane	144.1006	Strong reducing agent, contains multiple hydroxyl groups
6	Suberylglycine	254.0996	Moderate reducing agent, presence of amine and carboxyl groups
7	D-Tryptophan	204.0875	Strong reducing agent, indole structure with nitrogen
8	Methyl N-methylanthranilate	188.0688	Weak reducing properties, mainly an antimicrobial compound
9	Axisothiocyanate 3	264.1778	Weak reducing properties, primarily a defense compound
10	Buthionine sulfoximine	245.093	Weak reducing properties, involved in glutathione metabolism
11	3-furanmethanol glucoside	283.0786	Strong reducing agent due to glucoside and hydroxyl groups
12	N-acetyl-L-2-amino-6-oxopimelate	254.0999	Moderate reducing agent, presence of amine and carboxyl groups
13	Fospropofol	293.1106	Weak reducing properties, mainly a metabolic compound
14	Droxidopa	244.0944	Strong reducing agent, presence of hydroxyl groups
15	2-hydroxy-3-carboxy-6-oxo-7-methylocta-2,4-dienoate	251.0524	Moderate reducing agent, presence of hydroxyl and carboxyl groups
16	N5-(4-methoxybenzyl)glutamine	266.1269	Weak reducing properties, primarily involved in metabolic processes
17	2-hexylbenzothiazole	222.1037	Weak reducing properties, mainly a defense compound
18	Maculosin	260.0896	Moderate reducing agent, contains amine groups
19	N-carboxyacetyl-D-phenylalanine	254.0897	Moderate reducing agent, presence of carboxyl and amine groups
20	Alitame	331.1525	Moderate reducing agent, presence of multiple functional groups

Table 2. Metabolites identified in the pitcher fluid of *N. ventrata* by LC-HRMS analysis and their reducing properties.

Serial number	Name of the compound	Mass-to-charge ratio (m/z)	Major class
1	Evoxanthidine	270.0763	Phenolic Compound
2	Sarmentosin	275.0999	Alkaloid
3	3beta,6beta-Dihydroxynortropane	144.1006	Alkaloid
4	D-Tryptophan	204.0875	Amino Acid Derivative
5	3-furanmethanol glucoside	283.0786	Glucoside
6	Droxidopa	244.0944	Catecholamine

Table 3. Strong reducing agents identified in the pitcher fluid of *N. ventrata* by LC-HRMS analysis categorized by major classes.

concentration of 6 µg/mL, the AgNPs reduced biofilm formation to 18.3% of that observed in untreated controls. This significant decrease indicates the biosynthesized AgNPs have capability to disrupt early biofilm formation. When the concentration was increased to 12 µg/mL,, the biofilm biomass was further reduced to 6.5%, suggesting an enhanced disruption of biofilm structure and function. The most substantial disruption was observed at 24 µg/mL, where biofilm formation reduced to only 2.5% of the control, highlighting the strong antibiofilm properties of AgNps at higher concentrations. Fluorescence microscopy results further demonstrated that AgNPs effectively disrupted the structural integrity of PAO1 biofilms. A marked reduction in biofilm formation was observed at all tested concentrations (6 µg/mL, 12 µg/mL, and 24 µg/mL) compared to the control, highlighting the potent biofilm-inhibitory effect of AgNPs (Fig. 11). In this study, we successfully synthesized silver nanoparticles using *N. ventrata* and demonstrated their significant antibiofilm inhibitory activity. These findings are consistent with previous research that highlights the antibiofilm efficacy of silver nanoparticles synthesized through various biological methods. For instance, silver nanoparticles prepared using the aqueous extract of *Zataria multiflora* have been reported to exhibit substantial biofilm inhibitory activity. Similarly, *Solibacillus isronensis* has shown potent biofilm inhibition against *Escherichia coli* and *Pseudomonas aeruginosa*. Moreover, Tilank et al. described the biofilm inhibition capabilities of various phyto-mediated silver nanoparticles, further corroborating our results. These collective findings reinforce the potential of biologically synthesized silver nanoparticles as effective agents for biofilm inhibition[46–48]. The AgNPs demonstrated significant antibacterial activity and were effective in inhibiting bacterial biofilm formation. This antibacterial effect is enhanced by the presence of certain antibacterial compounds in the pitcher fluid that attach to the AgNPs. Notably, Methyl N-methylanthranilate and Axisothiocyanate 3, identified in the LC-HRMS analysis, are known for their strong antimicrobial properties. Methyl N-methylanthranilate is effective against microbial infections, while Axisothiocyanate 3 contributes to the plant's defence against pests and pathogens. These compounds, when adsorbed onto AgNPs, likely enhance the nanoparticles' ability to disrupt bacterial cell walls and inhibit biofilm formation, leading to bacterial cell death. Collectively, these results suggest that the biosynthesized AgNPs hold significant potential for use in

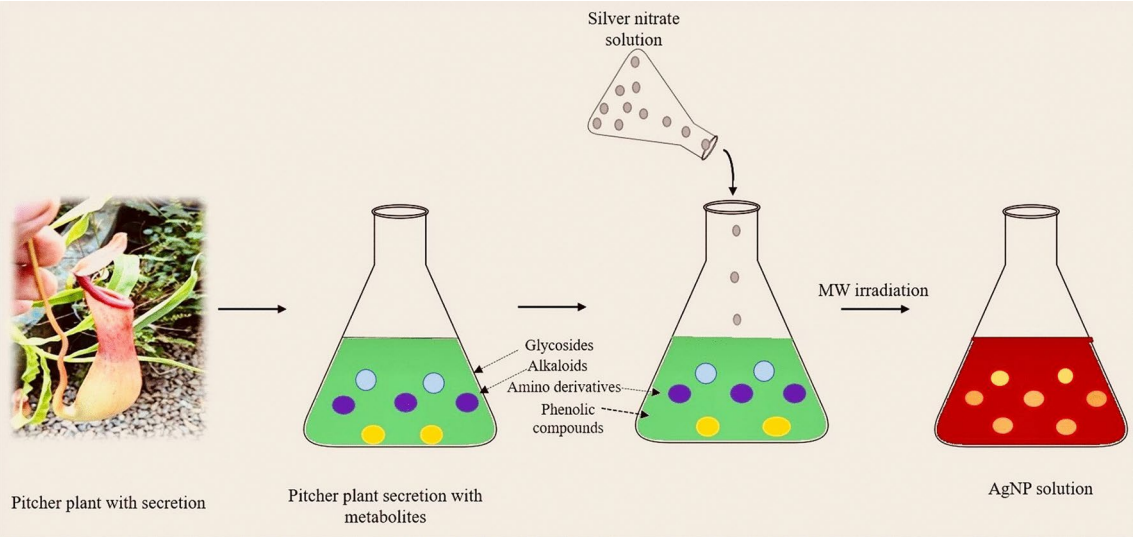

Fig. 9. Schematic representation of the formation of AgNPs using microwave-assisted (MW) synthesis, facilitated by the strong reducing agents present in the pitcher secretion of the insectivorous plant *N. ventrata*.

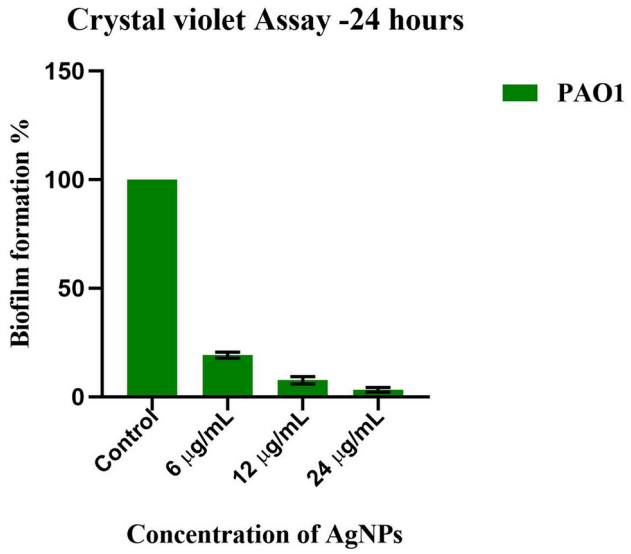

Fig. 10. Crystal Violet assay showing the percentage of bacterial biofilm formation in the presence of AgNPs (6 µg/mL, 12 µg/mL, and 24 µg/mL) in PAO1. Error bars represent standard error of Deviation .

coating applications on biomedical devices. By incorporating AgNPs into device coatings, it may be possible to reduce the risk of biofilm-associated infections, a common issue in medical implants and catheters. This could lead to improved patient outcomes by minimizing infection rates and enhancing the longevity of biomedical devices.

The antimicrobial and anticancer efficacy of AgNPs synthesized using *N. ventrata* secretion can be compared to those synthesized via other green methods. AgNPs synthesized using *Azadirachta indica* (neem) leaf extract have demonstrated significant antibacterial and anticancer activities, attributed to bioactive compounds like flavonoids and terpenoids[50]. Similarly, AgNPs produced using *Ocimum sanctum* (holy basil) leaf extract exhibit potent antimicrobial efficacy and selective cytotoxicity against cancer cells due to their unique surface properties and stability[51]. *Nepenthes ventrata* secretion offers a distinctive advantage because of its complex metabolic profile, including phenolic compounds, glycosides, and alkaloids, which enhance capping, stabilization, and functionalization of AgNPs. These unique properties may result in higher efficacy and broader-spectrum activity compared to nanoparticles synthesized using other plant extracts. Additionally, microwave-assisted synthesis with *N. ventrata* secretion accelerates nanoparticle formation, making the process time-efficient and environmentally friendly, thus distinguishing it from conventional green synthesis methods.

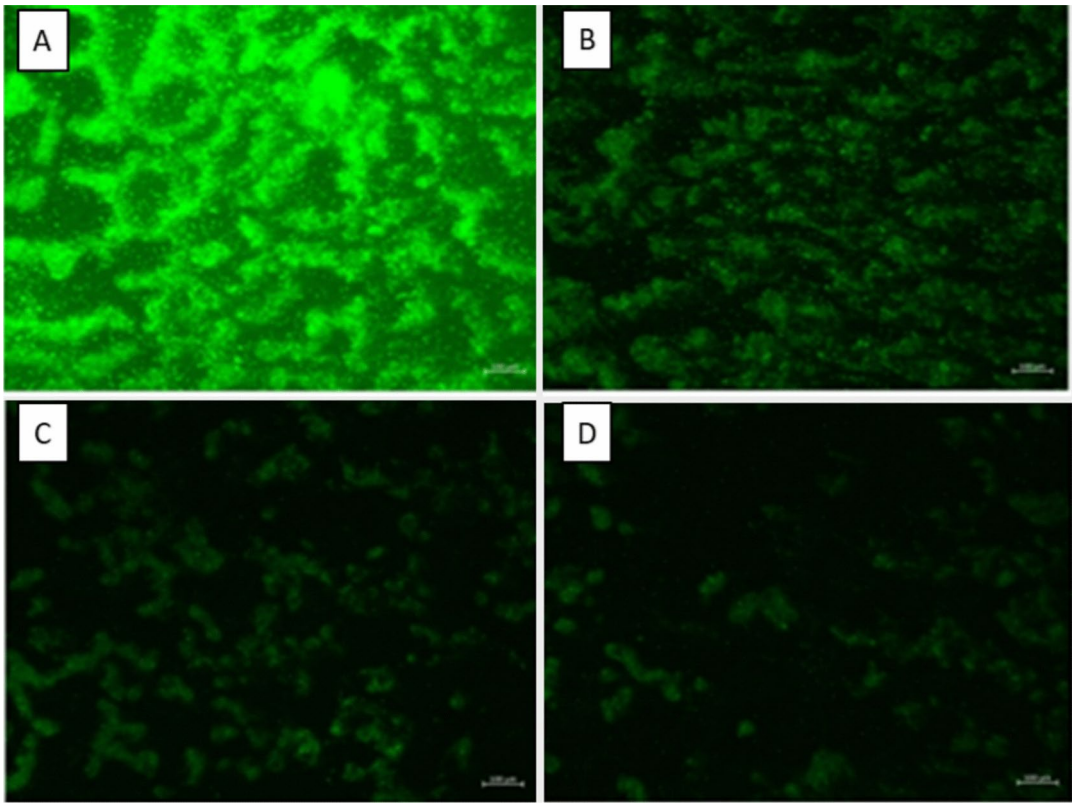

Fig. 11. Fluorescent Microscopic Imaging of PAO1 Biofilms—(**A**) Untreated Control. (**B**–**D**) indicate biofilm formation in the presence of 6 µg/mL, 12 µg/mL, and 24 µg/mL of AgNPs, respectively. The panels (**B**–**D**) show a decrease in fluorescence intensity, indicating fewer cells in the biofilm with increasing NP concentration, confirming high antibiofilm activity.

Green synthesized AgNPs, typically synthesized using plant extracts are often reported to exhibit enhanced antimicrobial and anticancer activities. For instance, AgNPs synthesized using *Azadirachta indica* extract exhibit potent antimicrobial activity against Gram-positive and Gram-negative bacteria[51]. Similarly, AgNPs synthesized using *Citrus sinensis* peel extract demonstrated significant cytotoxicity against MCF-7 breast cancer cells, attributed to the high flavonoid content[52]. In another study, fungal filtrates were employed for AgNPs synthesis, yielding strong antifungal activity and nanopesticide properties. AgNPs synthesized using *Chlorella vulgaris* extract showed broad-spectrum antimicrobial effects but moderate anticancer properties, likely due to differences in bioactive metabolites[53]. The rich metabolite profile of *N. ventrata*, particularly its phenolic compounds and glycosides, may enhance both antimicrobial and anticancer efficacy. These comparisons underscore the competitive advantages of using *N. ventrata* as a reducing and stabilizing agent in green synthesis.

Cytotoxicity assay of AgNPS

The cytotoxic effects of silver nanoparticles synthesized from *N. ventrata* pitcher fluids were evaluated using the MTT assay on A549 lung cancer cells. The cells were treated with various concentrations of NPs (10–50 µg/ml) for 24 h, and cell viability was assessed. At 10 µg/ml, the cell viability was 87.40%, indicating minimal cytotoxicity. Increasing concentrations of NPs showed a dose-dependent decrease in cell viability: 71.48% at 20 µg/ml, 59.15% at 30 µg/ml, 45.62% at 40 µg/ml, and 25.52% at 50 µg/ml. The IC_{50} value was determined to be 36.596 ± 0.710 µg/ml (Fig. 12). Morphological changes were also observed: control cells displayed normal morphology with intact membranes, whereas treated cells (30 and 40 µg/ml) exhibited significant morphological changes such as shrinkage, membrane blabbing, and distorted shapes, indicative of cytotoxic effects. The AgNPs also displayed significant anticancer activity, inducing apoptosis in A549 lung cancer cells. This effect can be linked to the bioactive compounds in the pitcher fluid with known anticancer properties. Compounds such as Evoxanthidine**,** Hypoglycin B**,** and Sarmentosin were identified in the LC-HRMS analysis. Evoxanthidine is known for its defensive properties that could help induce apoptosis and inhibit cancer cell proliferation. Hypoglycin B, known for its role in metabolic regulation, may disrupt cancer cell metabolism, leading to cell death. Sarmentosin contributes to the formation of defensive secondary metabolites that could enhance the cytotoxic effects of AgNPs against cancer cells. These compounds, when associated with AgNPs, likely amplify their effectiveness in targeting and killing cancer cells.

The green synthesis of AgNPs using *Phoenix dactylifera*, *Salvia*, and *Derris trifoliata* has demonstrated a moderate level of cytotoxicity in the MTT assay on A549 cells, a commonly studied lung cancer cell line. This observation is consistent with our previous findings on the cytotoxic effects of AgNPs derived from *N. ventrata*

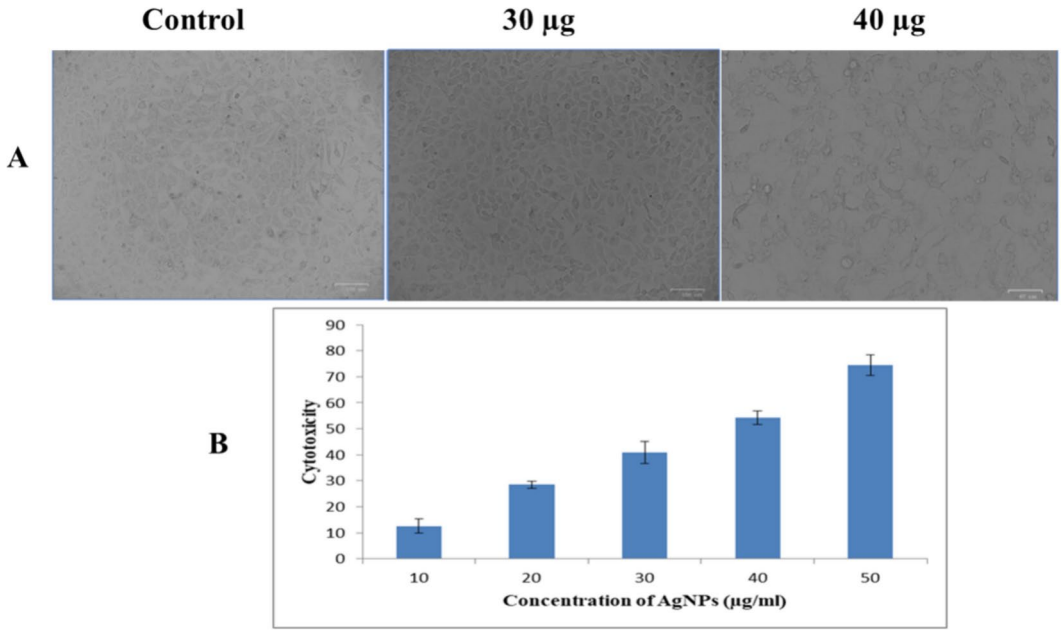

Fig. 12. Cytotoxicity Assay of AgNPs: (**A**) Cytotoxicity displayed by the control and samples at 30 µl and 40 µl concentrations. (**B**) Graphical representation of the cytotoxicity exhibited by AgNPs at various concentrations.

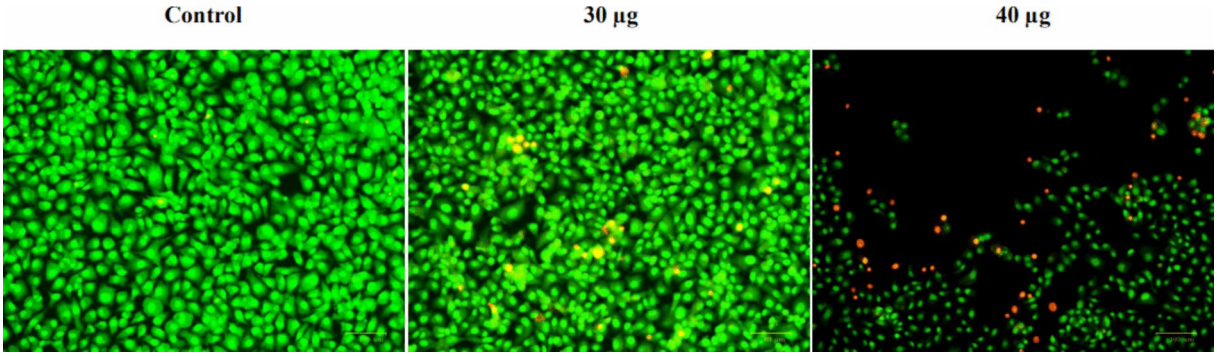

Fig. 13. Apoptotic Staining of Lung Cancer A549 Cells—Apoptotic staining of control and AgNPs-treated (30 µg and 40 µg) Lung Cancer A549 cells after 24 h of treatment. The images depict the apoptotic effects of AgNPs on the cells, demonstrating increased apoptosis with higher AgNP concentrations.

in similar assays. The alignment between these results highlights the inherent cytotoxic potential of biologically synthesized AgNPs across different plant sources. This consistency further emphasizes their potential as promising agents for cancer treatment, especially in targeting cancerous cells through eco-friendly synthesis methods[54–56].

Apoptotic induction assay

The apoptotic effects of the NPs were further assessed using the acridine orange/ethidium bromide (AO/EB) dual staining method. This method differentiates between viable, early apoptotic, late apoptotic, and necrotic cells based on fluorescence emission and chromatin condensation. Fluorescence microscopy observations revealed that control cells showed uniform bright green nuclei, indicating viability (Fig. 13). Early apoptotic cells (30 µg/ml) displayed green nuclei with perinuclear chromatin condensation, while late apoptotic cells (40 µg/ml) exhibited orange to red nuclei with condensed or fragmented chromatin. The presence of necrotic cells was minimal, suggesting apoptosis as the primary mode of cell death induced by the NPs. The apoptosis-inducing potential of biosynthesized silver nanoparticles (AgNPs) from various plant sources, such as *Moringa oleifera*, *Gossypium hirsutum*, and *Pinus roxburghii*, offers a promising platform for exploring nanoparticle-mediated therapeutic strategies. Several studies have demonstrated that AgNPs synthesized through green methods using plant extracts exhibit significant cytotoxic activity, particularly in cancer cell lines, by inducing apoptosis, the programmed cell death crucial for eliminating damaged or unwanted cells[57]. In particular, the bioactive compounds found in these plant extracts play a dual role in both the synthesis and stabilization of

AgNPs while enhancing their biological activity. For instance, *Moringa oleifera* has been shown to contain various phytochemicals, such as flavonoids and phenolic compounds, which can serve as reducing agents in the synthesis of AgNPs. These bio-reduced nanoparticles not only possess potent antioxidant properties but also demonstrate an ability to trigger apoptosis in cancer cells through pathways that involve reactive oxygen species (ROS) generation, mitochondrial dysfunction, and activation of caspases[58]. Similarly, *Gossypium hirsutum* and *Pinus roxburghii* extracts have also been reported to facilitate the synthesis of AgNPs with strong apoptotic potential. The secondary metabolites present in these plants can modulate cellular pathways, leading to increased oxidative stress and subsequent apoptosis in cancer cells. This growing body of evidence supports the utility of plant-mediated AgNPs as potential anticancer agents, providing a cost-effective and eco-friendly alternative to chemically synthesized nanoparticles[57,59]. The present study on the apoptosis-inducing potential of AgNPs biosynthesized from *Nepenthes ventrata* follows this trajectory, adding to the growing pool of evidence that plant-based synthesis of silver nanoparticles can yield potent anticancer agents. The phytochemicals present in *N. ventrata* may offer unique advantages in enhancing the efficacy and selectivity of AgNPs in triggering apoptotic pathways in malignant cells. This is consistent with previous findings from other plant-mediated AgNPs studies, further validating the role of phytochemicals in both nanoparticle synthesis and their bioactivity.

The comparative approach in using different plant sources for AgNPs biosynthesis underscores the importance of the phytochemical composition in influencing the biological properties of nanoparticles. By leveraging the unique secondary metabolites in *N. ventrata*, we aim to explore novel mechanisms of apoptosis induction, which could lead to the development of more effective cancer therapies. The evidence provided by previous studies on *Moringa oleifera*, *Gossypium hirsutum*, and *Pinus roxburghii* strengthens the foundation of our work, offering valuable insights into the underlying principles governing the biological activity of biosynthesized AgNPs.

Radical scavenging properties

The radical scavenging properties of the synthesized AgNPs suggest their potential in neutralizing free radicals and protecting cells from oxidative stress. Compounds such as D-Tryptophan**,** Buthionine Sulfoximine**,** and Fospropofol identified in the pitcher fluid are known for their antioxidant activities. D-Tryptophan is involved in nitrogen metabolism and has antioxidant properties. Buthionine Sulfoximine plays a role in glutathione metabolism, a critical pathway for maintaining cellular redox balance. Fospropofol supports antioxidative functions through its involvement in biochemical pathways. These molecules, when associated with AgNPs, enhance the nanoparticles' ability to scavenge free radicals, thereby protecting cells from oxidative damage.

Silver nanoparticles synthesized using natural extracts exhibit significant antioxidant activities, irrespective of their biological origin, whether derived from plants or other organisms[60–64]. This is primarily due to the presence of bioactive compounds in these extracts, which not only act as reducing and stabilizing agents in nanoparticle synthesis but also contribute to their enhanced antioxidant properties[65]. Here the DPPH assay shows a IC_{50} value of 25 µg. In particular, plant-derived AgNPs have garnered considerable attention for their potent antioxidant activity. For instance, AgNPs synthesized from *Holigarna arnottiana* have demonstrated strong free radical scavenging abilities, likely due to the rich content of phenolic compounds and flavonoids in the plant extract. These compounds donate electrons to neutralize free radicals, thereby reducing oxidative stress, which is crucial in preventing cellular damage and promoting overall health[66]. Similarly, AgNPs synthesized from *Ficus racemosa* have shown high antioxidant potential. The bioactive components present in this plant, such as tannins and saponins, not only facilitate the green synthesis of AgNPs but also play a crucial role in enhancing their capacity to counteract oxidative damage. This makes them valuable for applications where oxidative stress is a key factor, such as in aging and cancer therapies[67]. AgNPs mediated by oleuropein, a phenolic compound found in olive leaves, and cumin extracts have also exhibited strong antioxidant properties. Oleuropein, known for its robust antioxidant activity, imparts these properties to AgNPs, making them particularly effective in neutralizing reactive oxygen species (ROS). Cumin-mediated AgNPs, rich in antioxidants like terpenes and phenolics, similarly show a high capacity for reducing oxidative stress[68,69]. The consistent high antioxidant activity of these plant-mediated AgNPs emphasize the potential of green-synthesized nanoparticles as both therapeutic and protective agents (Fig. 14). By leveraging the intrinsic bioactive compounds in plant extracts, these AgNPs not only offer eco-friendly synthesis but also deliver enhanced biological benefits, making them suitable candidates for use in pharmaceutical, cosmetic, and health-related applications.

The antioxidant activity of AgNPs synthesized using *N. ventrata* secretion likely involves multiple mechanisms for scavenging DPPH radicals, primarily driven by electron transfer and hydrogen atom transfer (HAT) processes. The bioactive metabolites present in the secretion, such as phenolic compounds, glycosides, and alkaloids, play a critical role in stabilizing and functionalizing the AgNPs. These compounds may donate electrons or hydrogen atoms to neutralize the unpaired electrons of DPPH radicals, converting them into a more stable, non-radical form[70]. Additionally, the surface properties of AgNPs, such as their small size and high surface area enhance their ability to interact with free radicals. The reactive oxygen species (ROS) generated on the surface of AgNPs could also contribute to the reduction of DPPH radicals through redox cycling[71]. Furthermore, the presence of capping agents derived from *N. ventrata* secretion ensures the stability of AgNPs, preventing aggregation and allowing optimal interaction with free radicals[72]. This multi-faceted scavenging mechanism underlines the high antioxidant potential of AgNPs synthesized using *N. ventrata*. By combining unique surface characteristics and the bioactive profile of the secretion, the synthesized nanoparticles exhibit enhanced efficacy in neutralizing oxidative stress, offering promising therapeutic applications.

Environmental toxicity studies

To address the concern regarding the toxicity profile of the biosynthesized AgNPs and their safety for applications, a toxicity assessment was conducted using the *Allium cepa* assay. This assay, widely recognized for its sensitivity in detecting genotoxic and cytotoxic effects, provided valuable insights into the safety profile of the

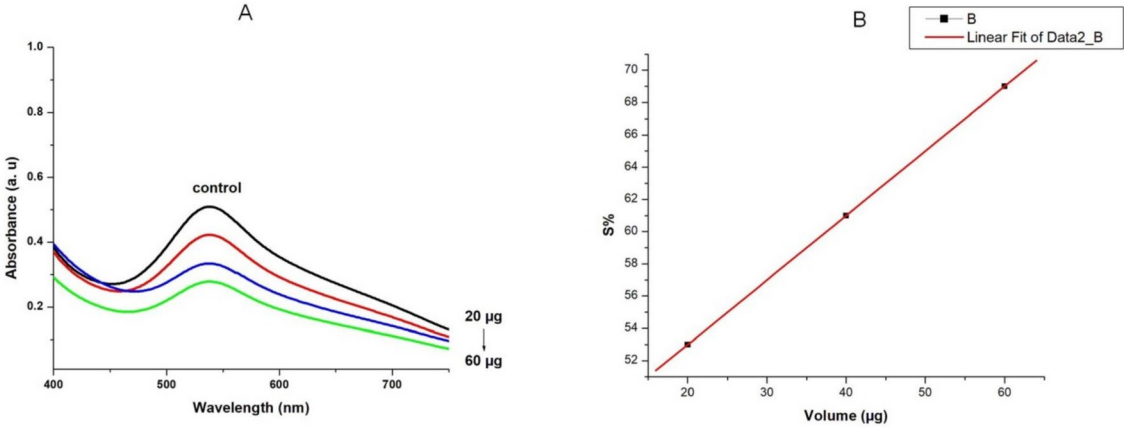

Fig. 14. DPPH assay (**A**) Scavenging activity (**B**) Calibration curve.

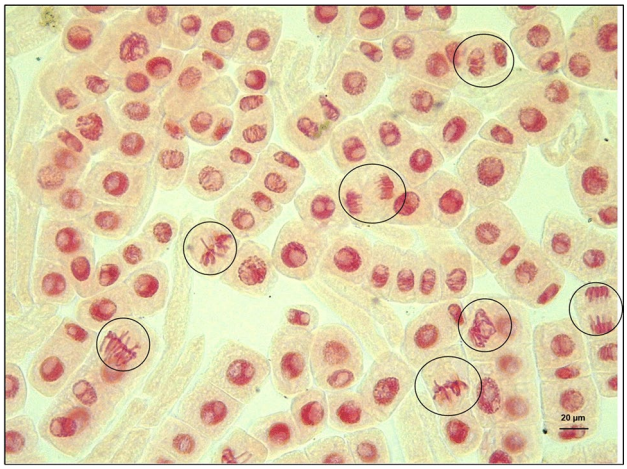

Fig. 15. Environmental Toxicity assay of AgNPs on *Allium cepa*.

synthesized AgNPs. The study revealed that AgNPs, at concentrations ranging from 100 µg to 500 µg, induced only minimal chromosomal aberrations, such as some sort of laggard chromosomes only which are marked in Fig. 15. These aberrations were quantified as a percentage relative to both control and experimental conditions (Table 4). Importantly, the Mitotic Index (MI) in the experimental groups showed no significant deviation from the control group, indicating the absence of substantial genotoxic or mito-depressive effects. This suggests that the AgNPs synthesized using *N. ventrata* secretions are biocompatible and exhibit minimal phytotoxicity. These findings are supported by previous studies, which have reported varying degrees of chromosomal aberrations induced by AgNPs[73–75]. The present study demonstrates that the green-synthesized AgNPs induce aberrations at much lower percentages compared to chemically synthesized counterparts, reinforcing the potential safety of the biosynthesized nanoparticles[75–81].

Conclusion

In conclusion, the synthesis of AgNPs using *Nepenthes ventrata* pitcher fluid has demonstrated the potential for creating biologically active nanoparticles with enhanced properties. Through comprehensive chemical characterizations, including UV–Vis, FTIR, TEM, zeta potential, and DLS analyses, the formation of stable, spherical AgNPs with a size range of 20–30 nm was confirmed. These AgNPs exhibited significant antibacterial, antibiofilm anticancer, and radical scavenging activities, which can be attributed to the bioactive compounds present in the pitcher fluid, such as Methyl N-methylanthranilate, Axisothiocyanate 3, Evoxanthidine, Hypoglycin B, Sarmentosin, D-Tryptophan, Buthionine Sulfoximine, and Fospropofol. The synergistic effects between these phytochemicals and the AgNPs offer promising potential for applications in antimicrobial treatments, cancer therapy, and antioxidant therapies. However, further research is required to fully understand the underlying mechanistic pathways and to optimize the therapeutic use of these biogenic nanoparticles for clinical applications. This study highlights the untapped potential of *N. ventrata* as a sustainable and natural source for the production of bioactive AgNPs, paving the way for future advancements in green nanotechnology.

Treatment	Concentration (µL)	Mitotic Index (% ± SD)	Chromosomal aberration (% ± SD)
Control (Distilled water)	100 µl	10.21 ± 0.20	NIL
	200 µl	10.69 ± 0.20	NIL
	300 µl	11.13 ± 0.20	NIL
	400 µl	12.29 ± 0.20	NIL
	500 µl	13.24 ± 0.20	NIL
Experiment (Biosynthesised AgNPs)	100 µl	10.51 ± 0.03	NIL
	200 µl	12.24 ± 0.03	NIL
	300 µl	12.8 ± 0.03	NIL
	400 µl	13.32 ± 0.03	NIL
	500 µl	14.24 ± 0.03	3 ± 0.04

Table 4. Mitotic index Vs Percentage of chromosomal aberration.

Data availability

All data generated or analysed during this study are included in this published article [and its supplementary information files].

Received: 23 September 2024; Accepted: 4 February 2025
Published online: 13 February 2025

References

1. Brewer, J. S. et al. Carnivory in plants as a beneficial trait in wetlands. *Aquat. Bot.* **94**, 62–70 (2011).
2. Ellison, A. M. & Gotelli, N. J. Evolutionary ecology of carnivorous plants. *Trends Ecol. Evol.* **16**, 623–629 (2001).
3. Méndez, M. & Karlsson, P. S. Costs and benefits of carnivory in plants: Insights from the photosynthetic performance of four carnivorous plants in a subarctic environment. *Oikos* **86**, 105–112 (1999).
4. Ornduff, R. & Darwin,. Darwin's botany. *Taxon* **33**, 39–47 (1984).
5. Mithöfer, A. Carnivorous pitcher plants: Insights in an old topic. *Phytochemistry* **72**, 1678–1682 (2011).
6. Stein, B. Insectivorous plants by Charles Darwin. (London, John Murray, Albemarle Street, 1875.). *Österreichische Botanische Zeitschrift* **26**, 61–67 (1876).
7. Adamec, L., Matušíková, I. & Pavlovič, A. Recent ecophysiological, biochemical and evolutional insights into plant carnivory. *Ann. Bot.* **128**, 241–259 (2021).
8. Sanusi, S. B., Abu-Bakar, M. F., Mohamed, M., Sabran, S. F. & Mainasara, M. M. Ethnobotanical, phytochemical, and pharmacological properties of nepenthes species: a review. *Asian J. Pharmaceut. Clin. Res.* **10**, 16–19 (2017).
9. Bhau, B. S. et al. Green synthesis of gold nanoparticles from the leaf extract of nepenthes Khasiana and antimicrobial assay. *Adv. Mater. Lett.* **6**, 55–58 (2015).
10. Dhamecha, D., Jalalpure, S. & Jadhav, K. *Nepenthes khasiana* mediated synthesis of stabilized gold nanoparticles: Characterization and biocompatibility studies. *J. Photochem. Photobiol. B Biol.* **154**, 108–117 (2016).
11. Majeed, S. & Mahmad, A. Biosynthesis of silver nanoparticles using Nepenthes Spp. and its bactericidal effect. *Der Pharma Chemica* **8**(19), 279–282 (2016).
12. Rajan, P. P. et al. Antibiofilm potential of gallic acid against Klebsiella pneumoniae and Enterobacter hormaechei: In-vitro and in-silico analysis. *Biofouling* **39**, 948–961 (2023).
13. Mini, M., Jayakumar, D. & Kumar, P. In-silico and in-vitro assessment of the antibiofilm potential of azo dye, carmoisine against Pseudomonas aeruginosa. *J. Biomol. Struct. Dyn.* **42**, 6700–6710 (2024).
14. Bogachev, M. I. et al. Fast and simple tool for the quantification of biofilm-embedded cells sub-populations from fluorescent microscopic images. *PLOS ONE* **13**, e0193267 (2018).
15. Popovic, S., Arsenijevic, N. & Baskic, D. In vitro assay for the quantitative measurement of apoptotic lymphocytes phagocytosis by peripheral blood monocytes. *Acta Physiol. Hung.* **93**, 325–333 (2006).
16. Ahmed, B., Shahid, M., Khan, M. S. & Musarrat, J. Chromosomal aberrations, cell suppression and oxidative stress generation induced by metal oxide nanoparticles in onion (Allium cepa) bulb†. *Metallomics* **10**, 1315–1327 (2018).
17. Roy, P., Das, B., Mohanty, A. & Mohapatra, S. Green synthesis of silver nanoparticles using Azadirachta indica leaf extract and its antimicrobial study. *Appl. Nanosci.* **7**, 843–850 (2017).
18. Bagherzade, G., Tavakoli, M. M. & Namaei, M. H. Green synthesis of silver nanoparticles using aqueous extract of saffron (*Crocus sativus* L.) wastages and its antibacterial activity against six bacteria. *Asian Pacific J. Trop. Biomed.* **7**, 227–233 (2017).
19. Sadeghi, B. & Gholamhoseinpoor, F. A study on the stability and green synthesis of silver nanoparticles using *Ziziphora tenuior* (*Zt*) extract at room temperature. *Spectrochimica Acta Part A Mol. Biomol. Spectroscopy* **134**, 310–315 (2015).
20. Paosen, S., Saising, J., Wira Septama, A. & Piyawan Voravuthikunchai, S. Green synthesis of silver nanoparticles using plants from Myrtaceae family and characterization of their antibacterial activity. *Mater. Lett.* **209**, 201–206 (2017).
21. Rupiasih, N. N., Aher, A., Gosavi, S. & Vidyasagar, P. B. Green synthesis of silver nanoparticles using latex extract of Thevetia peruviana: A novel approach towards poisonous plant utilization. In *Recent Trends in Physics of Material Science and Technology* (eds Gaol, F. L. et al.) 1–10 (Springer, 2015). https://doi.org/10.1007/978-981-287-128-2_1.
22. Shrestha, S., Wang, B. & Dutta, P. Nanoparticle processing: Understanding and controlling aggregation. *Adv. Colloid Interface Sci.* **279**, 102162 (2020).
23. Ling, D., Hackett, M. J. & Hyeon, T. Surface ligands in synthesis, modification, assembly and biomedical applications of nanoparticles. *Nano Today* **9**, 457–477 (2014).
24. Yang, H.-M., Park, C. W., Park, S. & Kim, J.-D. Cross-linked magnetic nanoparticles with a biocompatible amide bond for cancer-targeted dual optical/magnetic resonance imaging. *Colloids Surfaces B Biointerfaces* **161**, 183–191 (2018).
25. Dorjnamjin, D., Ariunaa, M. & Shim, Y. K. Synthesis of silver nanoparticles using hydroxyl functionalized ionic liquids and their antimicrobial activity. *Int. J. Mol. Sci.* **9**, 807–820 (2008).
26. Uznanski, P., Zakrzewska, J., Favier, F., Kazmierski, S. & Bryszewska, E. Synthesis and characterization of silver nanoparticles from (bis)alkylamine silver carboxylate precursors. *J. Nanopart. Res.* **19**, 121 (2017).

27. Titkov, A. I. et al. Synthesis of silver nanoparticles stabilized by carboxylated methoxypolyethylene glycols: the role of carboxyl terminal groups in the particle size and morphology. *J. Incl. Phenom Macrocycl. Chem.* **94**, 287–295 (2019).
28. Hassan, H. et al. Green-synthesised silver nanoparticles from pandan extract: Enhancing PPE effectiveness and sustainability in the post-COVID era. *J. Clust. Sci.* **35**, 2663–2680 (2024).
29. Almadiy, A. A. & Nenaah, G. E. Ecofriendly synthesis of silver nanoparticles using potato steroidal alkaloids and their activity against Phytopathogenic Fungi. *Braz. Arch. Biol. Technol.* **61**, e18180013 (2018).
30. Sadeghi, B. & Gholamhoseinpoor, F. A study on the stability and green synthesis of silver nanoparticles using *Ziziphora tenuior* (*Zt*) extract at room temperature. *Spectrochim. Acta Part A Mol. Biomol. Spectroscopy* **134**, 310–315 (2015).
31. de Matos, R. A. & Courrol, L. C. Biocompatible silver nanoparticles prepared with amino acids and a green method. *Amino Acids* **49**, 379–388 (2017).
32. Feng, P. C. & Patrick, S. J. Studies of the action of hypoglycin-a, an hypoglycaemic substance. *Br. J. Pharmacol. Chemother.* **13**, 125–130 (1958).
33. Novaković, A.R. *et al.* An insight into in vitro bioactivity of wild-growing puffball species Lycoperdon perlatum (Pers) 1796. *Food Feed Res.* **42**(1), 51–58 (datum objavljivanja).
34. Jiang, Z. et al. Sarmentosin induces autophagy-dependent apoptosis via activation of Nrf2 in hepatocellular carcinoma. *J. Clin. Transl. Hepatol.* **11**, 863–876 (2023).
35. Shaik, L. & Chakraborty, S. Sequential pulsed light and ultrasound treatments for the inactivation of Saccharomyces cerevisiae and PPO and the retention of bioactive compounds in sweet lime juice. *Foods* **13**, 1996 (2024).
36. de Andrade, S. A. L., de Oliveira, V. H. & Mazzafera, P. Metabolomics of Nutrient-Deprived Forest Trees. In *Monitoring Forest Damage with Metabolomics Methods* 235–265 (Wiley, 2024). https://doi.org/10.1002/9781119868750.ch9.
37. Martens, D. A. & Frankenberger, W. T. Metabolism of tryptophan in soil. *Soil Biol. Biochem.* **25**, 1679–1687 (1993).
38. Ma, Y., Shi, Q., He, Q. & Chen, G. Metabolomic insights into the inhibition mechanism of methyl *N*-methylanthranilate: A novel quorum sensing inhibitor and antibiofilm agent against *Pseudomonas aeruginosa*. *Int. J. Food Microbiol.* **358**, 109402 (2021).
39. Agrawal, A. A. & Kurashige, N. S. A role for isothiocyanates in plant resistance against the specialist herbivore Pieris rapae. *J. Chem. Ecol.* **29**, 1403–1415 (2003).
40. White, R. D., Norton, R. & Bus, J. S. The effect of buthionine sulfoximine, an inhibitor of glutathione synthesis, on hepatic drug metabolism in the male mouse. *Toxicol. Lett.* **23**, 25–32 (1984).
41. Ohana, P. et al. beta-Furfuryl-beta-glucoside: An endogenous activator of higher plant UDP-glucose:(1–3)-beta-glucan synthase : Biological activity, distribution, and in vitro synthesis. *Plant Physiol* **98**, 708–715 (1992).
42. Li, J. J. *Chemistry and Pharmacology of Drug Discovery* (Wiley, 2024).
43. Biswas, A. D., Catte, A., Mancini, G. & Barone, V. Analysis of L-DOPA and droxidopa binding to human β2-adrenergic receptor. *Biophys. J.* **120**, 5631–5643 (2021).
44. Agulló, L., Romero-Silva, M. J., Domenech, M. & Seeger, M. p-Cymene promotes its catabolism through the p-Cymene and the p-Cumate Pathways, activates a stress response and reduces the biofilm formation in Burkholderia xenovorans LB400. *PLOS ONE* **12**, e0169544 (2017).
45. Ts, S. et al. Secondary metabolite profiling using HR-LCMS, antioxidant and anticancer activity of *Bacillus cereus* PSMS6 methanolic extract: In silico and in vitro study. *Biotechnol. Rep.* **42**, e00842 (2024).
46. Stierle, A. C., Cardellina, J. H. & Strobel, G. A. Maculosin, a host-specific phytotoxin for spotted knapweed from Alternaria alternata. *Proc. Natl. Acad. Sci. USA* **85**, 8008–8011 (1988).
47. Auerbach, M. H., Locke, G. & Hendrick, M. E. Alitame. In *Alternative Sweeteners* (CRC Press, 2012).
48. Kamer, A. M. A., El Maghraby, G. M., Shafik, M. M. & Al-Madboly, L. A. Silver nanoparticle with potential antimicrobial and antibiofilm efficiency against multiple drug resistant, extensive drug resistant Pseudomonas aeruginosa clinical isolates. *BMC Microbiol.* **24**, 277 (2024).
49. Holubnycha, V. et al. Antimicrobial activity of two different types of silver nanoparticles against wide range of pathogenic bacteria. *Nanomaterials* **14**, 137 (2024).
50. Ahmed, S., Saifullah, Ahmad, M., Swami, B. L. & Ikram, S. Green synthesis of silver nanoparticles using Azadirachta indica aqueous leaf extract. *J. Radiat. Res. Appl. Sci.* **9**, 1–7 (2016).
51. Rana, A. et al. An investigation of antimicrobial activity for plant pathogens by green-synthesized silver nanoparticles using Azadirachta indica and Mangifera indica. *Physchem* **3**, 125–146 (2023).
52. Balashanmugam, P. & Kalaichelvan, P. T. Biosynthesis characterization of silver nanoparticles using Cassia roxburghii DC. aqueous extract, and coated on cotton cloth for effective antibacterial activity. *Int. J. Nanomed.* **10**, 87–97 (2015).
53. Barabadi, H. et al. Chapter 12—Bioengineered silver nanoparticles for antimicrobial therapeutics. In *Bioengineered Nanomaterials for Wound Healing and Infection Control* (eds Barabadi, H. et al.) 443–473 (Woodhead Publishing, 2023). https://doi.org/10.1016/B978-0-323-95376-4.00009-5.
54. Cyril, N., George, J. B., Joseph, L., Raghavamenon, A. C. & S, V. P. Assessment of antioxidant, antibacterial and anti-proliferative (lung cancer cell line A549) activities of green synthesized silver nanoparticles from Derris trifoliata. *Toxicol. Res.* **8**, 297–308 (2019).
55. Rajendran, R., Pullani, S., Thavamurugan, S., Radhika, R. & Lakshmi-Prabha, A. Green fabrication of silver nanoparticles from Salvia species extracts: Characterization and anticancer activities against A549 human lung cancer cell line. *Appl. Nanosci.* **13**, 2571–2584 (2023).
56. Farshori, N. N. et al. Green synthesis of silver nanoparticles using *Phoenix dactylifera* seed extract and its anticancer effect against human lung adenocarcinoma cells. *J. Drug Deliv. Sci. Technol.* **70**, 103260 (2022).
57. Al-kawmani, A. A. et al. Apoptosis-inducing potential of biosynthesized silver nanoparticles in breast cancer cells. *J. King Saud Univ. Sci.* **32**, 2480–2488 (2020).
58. Vasanth, K., Ilango, K., MohanKumar, R., Agrawal, A. & Dubey, G. P. Anticancer activity of *Moringa oleifera* mediated silver nanoparticles on human cervical carcinoma cells by apoptosis induction. *Colloids Surfaces B Biointerfaces* **117**, 354–359 (2014).
59. Kanipandian, N., Li, D. & Kannan, S. Induction of intrinsic apoptotic signaling pathway in A549 lung cancer cells using silver nanoparticles from *Gossypium hirsutum* and evaluation of *in vivo* toxicity. *Biotechnol. Rep.* **23**, e00339 (2019).
60. Ajaykumar, A. P. et al. Green synthesis of silver nanoparticles using the leaf extract of the medicinal plant, Uvaria narum and its antibacterial, antiangiogenic, anticancer and catalytic properties. *Antibiotics* **12**, 564 (2023).
61. Ajaykumar, A. P. et al. A novel approach for the biosynthesis of silver nanoparticles using the defensive gland extracts of the beetle, Luprops tristis Fabricius. *Sci. Rep.* **13**, 10186 (2023).
62. Ajaykumar, A. P. et al. A bio-inspired approach for the synthesis of few-layer graphene using beetle defensive gland extract. *RSC Adv.* **14**, 5729–5739 (2024).
63. Sabira, O. et al. The chemical composition and antimitotic, antioxidant, antibacterial and cytotoxic properties of the defensive gland extract of the beetle, Luprops tristis fabricius. *Molecules* **27**, 7476 (2022).
64. Mathew, A. et al. Microwave-assisted greener synthesis of Silver nanoparticles using Entada rheedii leaf extract and investigation of its anticancer and antimicrobial properties. *Int. J. Nano Dimens.* **13**, 329–334 (2022).
65. Flieger, J. et al. Green synthesis of silver nanoparticles using natural extracts with proven antioxidant activity. *Molecules* **26**, 4986 (2021).
66. Ajaykumar, A. P. et al. Bio-fabricated silver nanoparticles from the leaf extract of the poisonous plant, Holigarna arnottiana: Assessment of antimicrobial, antimitotic, anticancer, and radical-scavenging properties. *Pharmaceutics* **15**, 2468 (2023).

67. Sabira, O. et al. From Ficus recemosa leaf galls to therapeutic silver nanoparticles: Antibacterial and anticancer applications. *Pharmaceutics* **16**, 1025 (2024).
68. Genc, N. et al. Biosynthesis, characterization and antioxidant activity of oleuropein-mediated silver nanoparticles. *Inorganic Nano-Metal Chem.* **51**, 411–419 (2020).
69. Keerthiga, N., Anitha, R., Rajeshkumar, S. & Lakshmi, T. Antioxidant activity of cumin oil mediated silver nanoparticles. *Pharmacognosy J.* **11**, 787–789 (2019).
70. Kedare, S. B. & Singh, R. P. Genesis and development of DPPH method of antioxidant assay. *J. Food Sci. Technol.* **48**, 412–422 (2011).
71. Ahmed, B., Hashmi, A., Khan, M. S. & Musarrat, J. ROS mediated destruction of cell membrane, growth and biofilms of human bacterial pathogens by stable metallic AgNPs functionalized from bell pepper extract and quercetin. *Adv. Powder Technol.* **29**, 1601–1616 (2018).
72. Yadav, S., Nadar, T., Lakkakula, J. & Wagh, N. S. Biogenic synthesis of nanomaterials: bioactive compounds as reducing, and capping agents. In *Biogenic Nanomaterials for Environmental Sustainability: Principles, Practices, and Opportunities* (eds Shah, M. P. et al.) 147–188 (Springer, 2024). https://doi.org/10.1007/978-3-031-45956-6_6.
73. Cvjetko, P. et al. Toxicity of silver ions and differently coated silver nanoparticles in Allium cepa roots. *Ecotoxicol. Environ. Saf.* **137**, 18–28 (2017).
74. Heikal, Y. M., Şuțan, N. A., Rizwan, M. & Elsayed, A. Green synthesized silver nanoparticles induced cytogenotoxic and genotoxic changes in *Allium* cepa L. varies with nanoparticles doses and duration of exposure. *Chemosphere* **243**, 125430 (2020).
75. Kumari, M., Mukherjee, A. & Chandrasekaran, N. Genotoxicity of silver nanoparticles in *Allium cepa*. *Sci. Total Environ.* **407**, 5243–5246 (2009).
76. Abdelsalam, N. R. et al. Genotoxicity effects of silver nanoparticles on wheat (*Triticum aestivum* L.) root tip cells. *Ecotoxicol. Environ. Saf.* **155**, 76–85 (2018).
77. Borovaya, M. et al. "Green" synthesis of Ag2S nanoparticles, study of their properties and bioimaging applications. *Appl. Nanosci.* **10**, 4931–4940 (2020).
78. Ghosh, M. et al. In vitro and in vivo genotoxicity of silver nanoparticles. *Mutation Res./Genetic Toxicol. Environ. Mutagenesis* **749**, 60–69 (2012).
79. Pesnya, D. S. Cytogenetic effects of chitosan-capped silver nanoparticles in the Allium cepa test. *Caryologia* **66**, 275–281 (2013).
80. Pesnya, D. S. & Romanovsky, A. V. Comparison of cytotoxic and genotoxic effects of plutonium-239 alpha particles and mobile phone GSM 900 radiation in the Allium cepa test. *Mutation Res./Genetic Toxicol. Environ. Mutagenesis* **750**, 27–33 (2013).
81. Yekeen, T. A. et al. Safety evaluation of green synthesized Cola nitida pod, seed and seed shell extract-mediated silver nanoparticles (AgNPs) using an Allium cepa assay. *J. Taibah Univ. Sci.* **11**, 895–909 (2017).

Acknowledgements

We sincerely acknowledge the PSG Institute of Coimbatore for their invaluable assistance with HR-TEM analysis. We also extend our gratitude to the SAIF, IIT Bombay, India, for their support in conducting the GC-HRMS and LC-HRMS analyses.

Author contributions

O.S.—Investigation, experimental work, writing of the original draft and data analysis, A.P.A.—Supervision, conceptualization, data curation, investigation, review and editing of the original draft. S.R.V.—Formal analysis, review, and editing. K.N.J.—data curation, review, and editing of the original draft. M.K.—experimental work, review, and editing. P.K. experimental work, writing of the original draft. P. V- experimental work, writing of the original draft. V. S. B- conceptualization, data curation. APA-, Data collection. A. V. R—Data collection, Formal analysis and writing of the original draft. Experimental work, formal analysis. K.V.Z—conceptualization and data curation.

Funding

This study did not receive any particular funding.

Declarations

Competing interests

The authors declare no competing interests.

Additional information

Supplementary Information The online version contains supplementary material available at https://doi.org/10.1038/s41598-025-89212-9.

Correspondence and requests for materials should be addressed to A.P.A. or K.N.J.